performance of devices [14,15]. This is especially important in PZT compositions in which the useful properties depend significantly on Zr/Ti ratio [1,14,16]. Over decades, tremendous amount of work has been dedicated to the processing of PZT with various preparation routes, one of which is a modified mixed oxide route [1,17,18]. In this route, the PZT is prepared by mixing precursor PZ with $PbTiO_3$ or PbO and TiO_2 powders [1,19,20]. This preparation route, as well as the B-site cations route, offers advantages in producing PZT with more controllable Zr/Ti ratio and desirable properties at lower sintering temperature without using excess PbO typically practiced in a more conventional mixed-oxide method [17,21,22]. The resulting PZT is, however, found to show variation in properties, probably caused in part by the stoichiometry of PZ precursor powders. In addition, earlier work by Reaney *et al* [23] reported that impure PZ specimen showed significantly inferior electrical properties as well as unclear TEM results in the antiferroelectric-ferroelectric (AFE-FE) phase boundary as a result of unreacted ZrO_2 phases. These reasons outlined have clearly indicated from both practical and fundamental viewpoints needs to obtain stoichiometric and better homogeneity PZ. To do such, different preparative methods have been introduced, such as chemical co-precipitation [24], sol-gel [25], precipitation of molecular precursors [26], citrate combustion [27], hydrothermal [28] and microemulsion method [29]. All these techniques are aimed at reducing the temperature of preparation of the compound even though they are more involved and complicated in approach than the solid-state reaction method. Moreover, high purity PZ powders are still not available in mass quantity and also expensive. So far, only limited attempts have been made to improve the yield of $PbZrO_3$ by optimizing calcination conditions [30-32]. The effects of applied dwell time and heating/cooling rates have not yet been studied extensively. It is our interest to explore a simple mixed oxide synthetic route for the production of PZ powders. This current work is focused only on processing of PZ powders, while PZ ceramic fabrication, as well as PZT powders and ceramics produced from the PZ powders obtained, will be presented in subsequent publications.

In this context, a systematic study of the reaction between lead oxide and zirconium oxide is of interest. The effect of calcination conditions (i.e. firing temperature, dwell time and heating/cooling rates) on the development of phase, morphology and particle size of lead zirconate powders is investigated in this connection. The potentiality of a vibro-milling technique as a significant time-saving method to obtain single-phase lead zirconate powders, at low temperature and with small particles is also examined.

2. Experimental procedure

The starting materials were commercially available lead oxide, PbO (JCPDS file number 77-1971) and zirconium oxide, ZrO_2 (JCPDS file number 37-1484) (Fluka, > 99% purity). The two oxide powders exhibited an average particle size in the range of 3.0 to 5.0 µm. $PbZrO_3$ powders were synthesized by the solid-state reaction of thoroughly ground mixtures of PbO and ZrO_2 powders that were milled in the required stoichiometric ratio. Instead of employing a ball-milling procedure (ZrO_2 media under ethanol for 24 h [30] or under a mixture of cyclohexane and deionized water for 12 h [31]), use was made of a McCrone vibro-milling technique [22,32,33]. In order to combine mixing capacity with a significant time saving, the milling operation was carried out for 0.5 h with corundum cylindrical media in isopropyl alcohol (instead of 8 h with zirconia media [32]). After drying at 120 ^{o}C for 2 h, the reaction of the uncalcined powders taking place during heat treatment was investigated by themogravimetric and differential thermal analysis (TG-DTA, Shimadzu), using a heating rate of 10 ^{o}C/min in air from room temperature up to 1000 ^{o}C. Based on the TG-DTA results, the mixture was calcined at various conditions, *i.e*. temperatures ranging from 700 to 900 ^{o}C, dwell times ranging from 1 to 5 h and heating/cooling rates ranging from 1 to 20 ^{o}C /min, in closed alumina crucible, in order to investigate the formation of lead zirconate.

Calcined powders were subsequently examined by room temperature X-ray diffraction (XRD; Siemens-D500 diffractometer), using Ni-filtered CuK$_{\alpha}$ radiation to identify the phases formed and optimum calcination conditions for the formation of $PbZrO_3$ powders. Crystallite sizes and lattice parameters in the calcined powders were estimated from XRD data [34,35]. Powder morphologies and particle sizes were directly imaged, using scanning electron microscopy (SEM; JEOL JSM-840A). The chemical compositions of the phase formed were elucidated by an energy-dispersive X-ray (EDX) analyzer with an ultra-thin window. EDX spectra were quantified with the virtual standard peaks supplied with the Oxford Instruments eXL software.

3. Results and discussion

The TG-DTA simultaneous analysis of a powder mixed in the stoichiometric proportions of $PbZrO_3$ is displayed in Fig. 1. In the temperature range from room temperature to ~ 150 ^{o}C, the sample shows both exothermic and endothermic peaks in the DTA curve, in consistent with a slight drop in weight loss at the same temperature range. These observations can be attributed to the decomposition of the organic species (most likely polyethylene from the milling jar) from the milling process. [22,33]. Corresponding to a large fall in sample weight (~ 4.5%), the other exotherm and endotherm are observed within 300 to 450 °C temperature range in the DTA curve. However, it is to be noted that there is no obvious interpretation of these peaks, although it is likely to correspond to a phase transformation of ZrO_2 precursor alloyed with PbO precursor reported by a number of workers [35-38]. In general, it is well established that there are a number of polymorphic forms of PbO and ZrO_2 stable at different temperatures and pressures [35,37]. However, in this work, the possibility of these phase transformations has not been investigated, since the overriding objective is to synthesize single phase $PbZrO_3$, irrespective of the polymorph in which it is stabilized.

Increasing the temperature up to ~ 1000 °C, the solid-state reaction occurred between PbO and ZrO_2 [29-32]. The broad exotherm from ~ 500 to 700 °C in the DTA curve represents that reaction, which is supported by a gradual decrease in sample weight over the same temperature range. Finally, a significantly drop in weight loss is also observed above 800 °C, that is associated with the DTA peaks at the same temperature range and may be attributed to the PbO volatilization commonly found in the lead-based perovskite systems [22,33,39]. These data were used together with those from literature [30-32] to assign the range of calcination temperatures for XRD investigation between 700 and 900 °C.

Therefore, to investigate the effect of calcination temperature on the phase development, the mixed powders were calcined for 2 h in air at various temperatures, up to 900 °C, followed by phase analysis using XRD. As shown in Fig. 2, for the uncalcined powder, only X-ray peaks of precursors PbO (▼) and ZrO_2 (•), which could be matched with JCPDS file numbers 77-1971 [40] and 37-1484 [41], respectively, are present, indicating that no reaction had yet been triggered during the milling process. It is seen that fine $PbZrO_3$ crystallites (★) were developed in the powder at a calcination temperature as low as 750 ^{o}C, accompanying with PbO and ZrO_2 as separated phases. This observation agrees well with those derived from the TG-DTA results and other workers [31,38]. As the temperature increased to 800 ^{o}C, the intensity of the perovskite-like $PbZrO_3$ peaks was further enhanced and became the predominant phase. Upon calcination at 850 ^{o}C, an essentially monophasic of $PbZrO_3$ phase is obtained. This PZ phase was indexable according to an orthorhombic perovskite-type structure with lattice parameters a = 823.1 pm, b = 1177 pm and c = 588.1 pm, space group *P2cb* (no. 32), in consistent with JCPDS file numbers 35-739 [42] and other investigators [24,30,43]. This study also shows that crystalline orthorhombic PZ is the only detectable phase in the powder, after calcination in the range 850-900 ^{o}C.

Having established the optimum calcination temperature, dwell times ranging from 1 to 5 h with constant heating/cooling rates of 5 ^{o}C/min were applied at 850 and 800 ^{o}C, as shown in Figs. 3 and 4, respectively. From Fig. 3, it can be seen that the single phase of $PbZrO_3$ (yield of 100% within the limitations of the XRD technique) was found to be possible in all powders calcined at 850 ^{o}C with dwell time ranging from 1 to 5 h. This is probably due to the effectiveness of vibro-milling and a carefully optimized reaction. However, in the work reported here, it is to be noted that single-phase of $PbZrO_3$ powders was also successfully obtained for a calcination temperature of 800 ^{o}C with dwell time of 3 h or more applied (Fig. 4). This was apparently a consequence of the enhancement in crystallinity of the $PbZrO_3$ phase with increasing dwell time. The appearance of PbO phase indicated that full crystallization has not occurred at relatively shorter calcination times. The observation that the dwell time effect may also play an important role in obtaining a single-phase perovskite product is also consistent with other similar systems [33,39,44].

Apart from the calcination temperature and dwell time, the effect of heating/cooling rates on the formation behaviour of $PbZrO_3$ was also investigated. Various heating/cooling rates ranging from 1 to 20 ^{o}C/min were selected for calcination conditions of 800 ^{o}C for 3 h (Fig. 5) and 850 ^{o}C for 1 h (Fig. 6). In this connection, it is shown that the yield of $PbZrO_3$ phase was not depending on heating/cooling rates, indicating that fast heating/cooling rates can lead to full crystallization of $PbZrO_3$ phase without time for the formation of minor phase or lead vaporization. The observation that faster heating/cooling rates are required for lead-based ferroelectrics is also consistent with other researchers [39,45,46]. It should be once again emphasized that these results clearly indicate effects of heating/cooling rates on the phase formation behavior of PZ powders. These parameters are very crucial for Pb-based compounds [22,47]. Usually, heating/cooling rates and dwell time show marked influences on phase formation behavior of other Pb-based compounds, such as PZT. It is of interest to observe that in PZ powders the heating/cooling rates do not show any effects on the behavior, while the dwell time only shows the effects on the particle agglomeration.

Based on the TG-DTA and XRD data, it may be concluded that, over a wide range of calcination conditions, single phase $PbZrO_3$ cannot be straightforwardly formed via a solid-state mixed oxide synthetic route, unless carefully designed calcination condition was performed. It is well documented that powders prepared by a conventional mixed oxide method have spatial fluctuations in their compositions. The extent of the fluctuation depends on the characteristics of the starting powders as well as the processing schedules [22,33,39]. The experimental work carried out here suggests that the optimal calcination conditions for single-phase $PbZrO_3$ (with impurities undetected by XRD technique) is 800 ^oC for 3 h or 850 ^oC for 1 h, with heating/cooling rates of 20 ^oC/min, which is closed to that of Puchmark *et al*. [30] (775 ^oC for 3 h with heating/cooling rates of 5 ^oC/min) but with significantly faster heating/cooling rates. Moreover, the formation temperature and/or dwell time for the production of $PbZrO_3$ powders observed in this work are also lower than those reported by Fang *et al*. [31] (900 ^oC for 1 h) and Lanagan *et al*. [32] (900 ^oC for 8 h).

Finally, the morphological changes in the $PbZrO_3$ powders formed by a mixed oxide are illustrated in Fig. 7 as a function of calcination temperatures, dwell times and heating/cooling rates, respectively. The influence of calcination conditions on particle size is given in Table 1. These particle size data were directly estimated from SEM micrographs. Even though these data are not precisely determined, they were shown to provide estimated comparison between different calcination conditions and to form a basis for other more detailed studies with use of a combination between TEM and particle size distribution analyzer. After calcinations at 800 to 900 ^oC, the powders seem to have similar morphology. In general, the particles are agglomerated and irregular in shape, with a substantial variation in particle size, particularly in samples calcined at higher temperatures or for longer dwell times. This observation is also similar to that of Mg_4 Nb_2O_9 powders synthesized by Ananta [48]. The results indicate that averaged particle size and degree of agglomeration tend to increase with calcination temperature and dwell time (Table 1). However, the smallest particle size (estimated from SEM micrographs to be ~ 250 nm) and the morphology of the calcined powders are about the same. It is also of interest to point out that no evidence has been obtained for the existence of the cubic or spherical shape morphology as that of the hydrothermally derived $PbZrO_3$ powders [28,49]. In additional, energy dispersive X-ray (EDX) analysis (Fig. 8) using a 20 nm probe on a large number of particles of the calcined powders confirms that the parent composition is $PbZrO_3$, in agreement with XRD results.

4. Conclusions

The methodology presented in this work provides a simple method for preparing perovskite $PbZrO_3$ powders via a solid-state mixed oxide synthetic route. By using optimal calcination conditions of 800 ^{o}C for 3 h or 850 ^{o}C for 1 h, with heating/cooling rates of 20 ^{o}C/min, the reproducible, low cost and fast process involving vibro-milling can provide high-purity perovskite $PbZrO_3$ powders with particle size ranging from 200–500 nm from inexpensive commercially available raw materials. The resulting $PbZrO_3$ powders consist of variety of agglomerated particle sizes, depending on calcination conditions. Finally, it should be emphasized that this work presents for the first time the effects of calcination conditions on the phase formation behavior of the PZ powders. These parameters clearly show significant influences on the processing of even simple binary system as PZ, and there is no doubt that they will show even more effects on other complicated materials such as PZT, PMN, PZN, PIN, and PMN-PT. The results on those systems are being produced and will be presented in future publications.

Acknowledgements

We thank the Thailand Research Fund (TRF), Graduate School and Faculty of Science, Chiang Mai University for all support.

References

[1] B. Jaffe, W.J. Cook, H. Jaffe, Piezoelectric Ceramics, Academic Press, London, 1971.

[2] F. Jona, G. Shirane, Ferroelectric Crystals, Dover Publications, New York, 1993.

[3] E. Sawaguchi, H. Maniwa, S. Hoshino, Phys. Rev. **83** (1951) 1078.

[4] G. Shirane, E. Sawaguchi, Y. Takagi, Phys. Rev. **84** (1951) 476.

[5] E. Sawaguchi, K. Kittaka, J. Phys. Soc. Jpn. **7** (1952) 336.

[6] V.J. Tennery, J. Am. Ceram. Soc. **49** (1966) 483.

[7] B.A. Scott. G. Burns, J. Am. Ceram. Soc. **55** (1972) 331.

[8] G. Shirane, S. Hoshino, Acta Crystallogr. **7** (1954) 203.

[9] B.P. Pokharel, D. Pandey, J. Appl. Phys. **86** (1999) 3327.

[10] T. Bongarn, G. Rujijanagul, S.J. Milne, Mater. Lett. **59** (2005) 1200.

[11] R.W. Whatmore, Ph.D. Thesis, Genville and Cauis College, Cambridge, 1976.

[12] K. Singh, Ferroelectrics, **94** (1989) 433.

[13] G.H. Haertling, J. Am. Ceram. Soc. **82** (1999) 797.

[14] A. J. Moulson, J. M. Herbert, Electroceramics, 2nd ed., Wiley, New York, 2003.

[15] K. Uchino, Piezoelectrics and Ultrasonic Applications, Kluwer, Deventer, 1998.

[16] K. Kakegawa, J. Mohri, T. Takahashi, H. Yamamura, S. Shirasaki, Solid State Commun. **24** (1977) 769

[17] A.I. Kingon, J.B. Clark, J. Am. Ceram. Soc. **66** (1983) 253.

[18] Y. Matsuo, H. Sasaki, J. Am. Ceram. Soc. **48** (1965) 289.

[19] O. Babushkin, T. Lindback, J.C. Lue, J.Y.M. Leblais, J. Eur. Ceram. Soc. **16** (1996) 1293.

[20] D.L. Hanky, J.V. Biggers, J. Am. Ceram. Soc. **12** (1951) 172.

[21] A. Garg, D.C. Agrawal, Mat. Sci. Eng. B **56** (1999) 46.

[22] R. Tipakontitikul, S. Ananta, Mater. Lett. **58** (2004) 449.

[23] I.M. Reaney, A. Glazounov, F. Chu, A. Bell, N. Setter, Brit. Ceram. Trans. **96** (1997) 217.

[24] E. E. Oren, E. Taspinar, A. C. Tas, J. Am. Ceram. Soc. **80** (1997) 2714.

[25] D. M. Ibrahim, H. W. Hennicke, Trans. J. Br. Ceram. Soc. **80** (1981) 18.

[26] A. S. Deshpande, Y. B. Khollam, A. J. Patil, S. B. Deshpande, H. S. Potdar, S. K. Date, Mater. Lett. **51** (2001) 161.

[27] Y. S. Rao, C. S. Sunandana, J. Mater. Sci. Lett. **11** (1992) 595.

[28] J. Y. Choi, C. H. Kim, D. K. Kim, J. Am. Ceram. Soc. **81** (1998) 1353.

[29] J. Fang, J. Wang, S.C. Ng, L.M. Gan, C.H. Quek, C.H. Chew, Mater. Lett. **36** (1998) 179.

[30] C. Puchmark, G. Rujijanagul, S. Jiansirisomboon, T. Tunkasiri, Ferroelectric Lett. **31** (2004) 1.

[31] J. Fang, J. Wang, S.C. Ng, L.M. Gan, C.H. Chew, Ceram. Inter. **24** (1998) 507.

[32] M. T. Lanagan, J. H. Kim, S. Jang and R. E. Newnham, J. Am. Ceram. Soc. **71** (1988) 311.

[33] S. Ananta, N.W. Thomas, J. Eur. Ceram. Soc. **19** (1999) 155.

[34] H. Klug, L.E. Alexander, X-Ray Diffraction Procedures for Polycrystalline and Amorphous Materials, 2nd ed., Wiley, New York, 1974.

[35] T. Aoyama, N. Kurata, K. Hirota, O. Yamaguchi, J. Am. Ceram. Soc. **78** (1995) 3163.

[36] S. Fushimi, T. Ikeda, J. Am. Ceram. Soc. **50** (1967) 129.

[37] W.E. Lee, W.M. Rainforth, Ceramic Microstructures: Property Control by Processing, Chapman & Hall, London, 1994.

[38] T.G. Deyneka, E.A. Vouk, V.M. Ishchuk, R.F. Ramakaeva, G.K. Volkova, T.E. Konstantinova, Funct. Mater. **11** (2004) 44.

[39] A. Udomporn, S. Ananta, Mater. Lett. **58** (2004) 1154.

[40] JCPDS-ICDD Card No. 77-1971. International Centre for Diffraction Data, Newtown Square, PA, 2002.

[41] JCPDS-ICDD Card No. 37-1484. International Centre for Diffraction Data, Newtown Square, PA, 2002.

[42] JCPDS-ICDD Card No. 35-739. International Centre for Diffraction Data, Newtown Square, PA, 2002.

[43] T. Tani, J.F. Li, D. Viehland, D.A. Payne, J. Appl. Phys. **75** (1994) 3017.

[44] S. Ananta, R. Brydson, N.W. Thomas, J. Eur. Ceram. Soc. **20** (2000) 2315.

[45] J. Ryu, J.J. Choi, H.E. Kim, J. Am. Ceram. Soc. **84** (2001) 902.

[46] C.E. Baumgartner, J. Am. Ceram. Soc. **71** (1988) C-350.

[47] A. Udomporn, K. Pengpat, S. Ananta, J. Eur. Ceram. Soc. **24** (2004) 185.

[48] S. Ananta, Mater. Lett. **58** (2004) 2530.

[49] H.K. Kim, M.S. Thesis, Seoul National University, Seoul, Korea, 1993.

TABLE CAPTION

Table 1 Effect of calcination conditions on particle size of $PbZrO_3$ powders.

FIGURE CAPTIONS

Fig. 1 TG-DTA curves for the mixture of PbO-ZrO_2 powders.

Fig. 2 XRD patterns of PZ powder calcined at various temperatures for 1 h with heating/cooling rates of 10 °C/min.

Fig. 3 XRD patterns of PZ powder calcined at 850 °C with heating/cooling rates of 10 °C/min for various dwell times.

Fig. 4 XRD patterns of PZ powder calcined at 800 °C with heating/cooling rates of 10 °C/min for various dwell times.

Fig. 5 XRD patterns of PZ powder calcined at 800 °C for 3 h with various heating/cooling rates.

Fig. 6 XRD patterns of PZ powder calcined at 850 °C for 1 h with various heating/cooling rates.

Fig. 7 SEM micrographs of the PZ powders calcined at (a) 850 °C/1h, (b) 850 °C/2h, (c) 900 °C/2h, with heating/cooling rates of 10 °C/min and (d) 850 °C/1h with heating/cooling rates of 20 °C/min.

Fig. 8 EDX analysis of PZ powders calcined at 850 °C for 1 h, with heating/cooling rates of 20 °C/min (some spectra indexed as C and Au come from coated electrode).

Table I Particle size range of $PbZrO_3$ powders calcined at various conditions

Temperature (°C)	**Dwell time (h)**	**Heating/cooling rates (°C/min)**	**Particle size range (mean)* (μm)**
800	3	3	0.35 – 0.60 (0.41)
800	3	5	0.15 – 1.00 (0.52)
850	1	3	0.30 – 1.00 (0.44)
850	1	5	0.30 – 0.80 (0.59)
850	1	10	0.25 – 0.70 (0.54)
850	1	20	0.30 – 0.80 (0.51)
850	2	10	0.25 – 1.20 (0.64)
900	2	10	0.35 – 1.50 (0.77)

* The estimated precision of the particle size is ± 10%

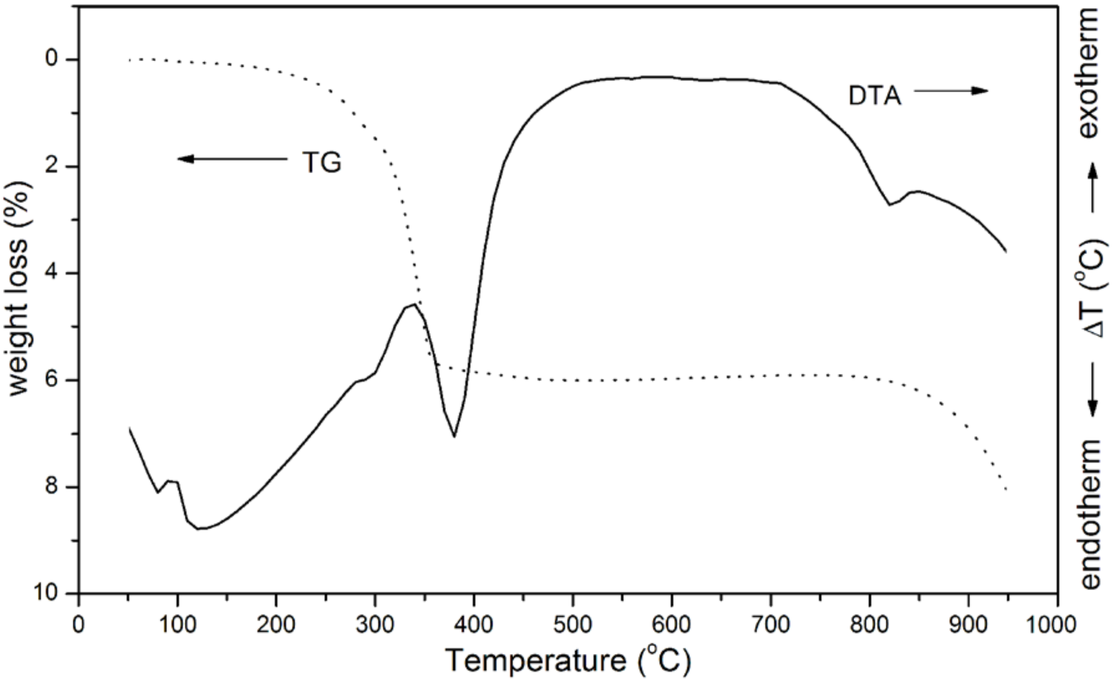
weight loss (%)
0
2
4
6
8
10
0
100
200
300
400
500
600
700
800
900
1000
Temperature (°C)
TG
DTA
endotherm
ΔT (°C)
exotherm

Fig. 1

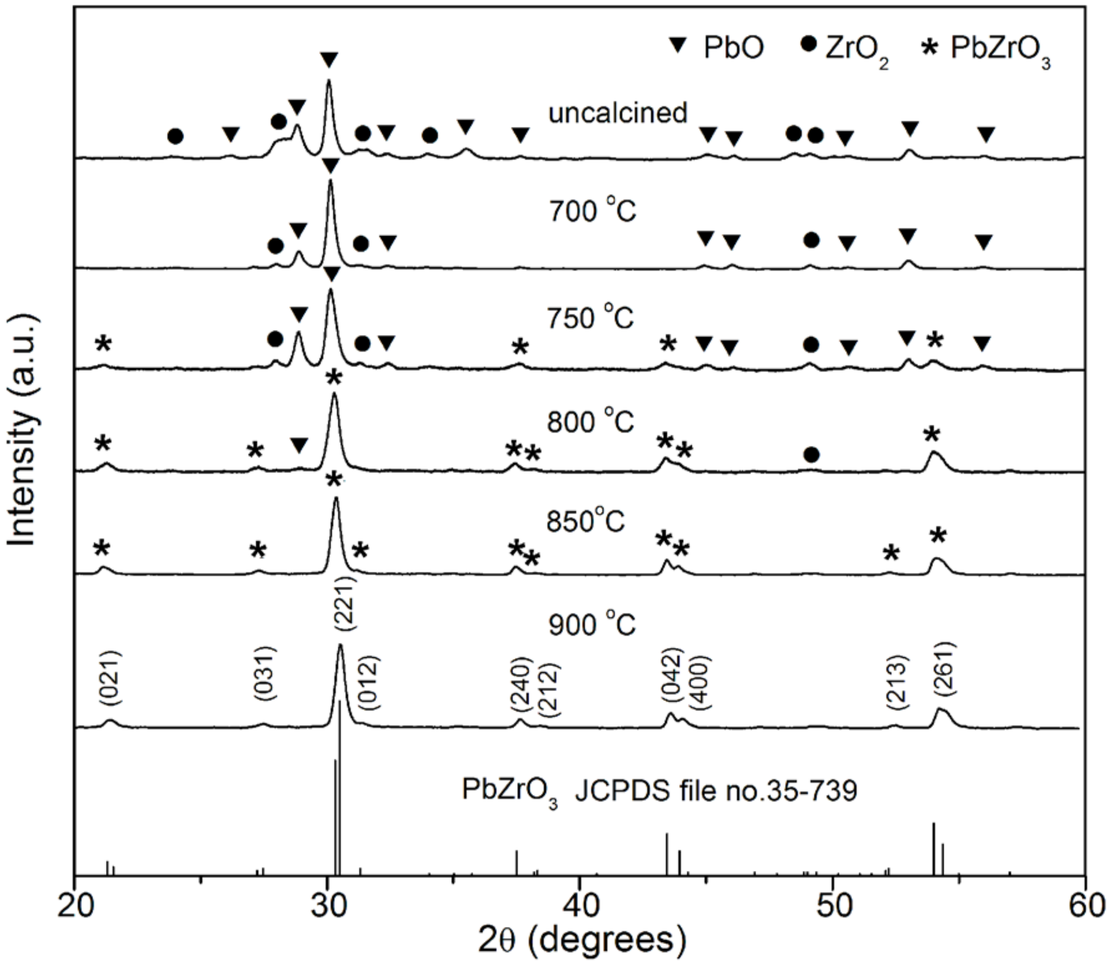
▼ PbO ● ZrO_2 * $PbZrO_3$
uncalcined
700 °C
750 °C
800 °C
850°C
900 °C
(021)
(031)
(221)
(012)
(240)
(212)
(042)
(400)
(213)
(261)
$PbZrO_3$ JCPDS file no.35-739
Intensity (a.u.)
2θ (degrees)
20
30
40
50
60

Fig. 2

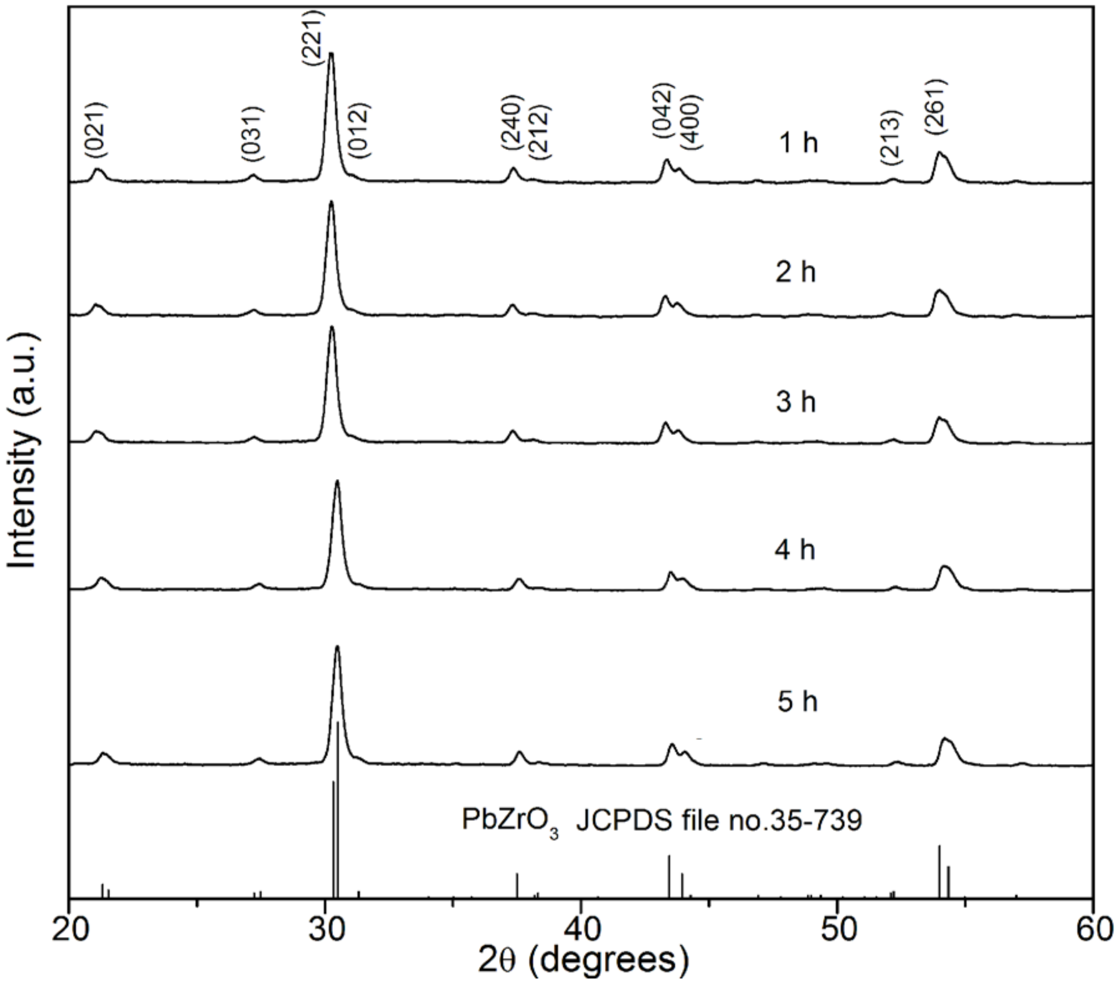
(021)
(031)
(221)
(012)
(240)
(212)
(042)
(400)
(213)
(261)
1 h
2 h
3 h
4 h
5 h
PbZrO$_3$ JCPDS file no.35-739
Intensity (a.u.)
2θ (degrees)
20
30
40
50
60

Fig. 3

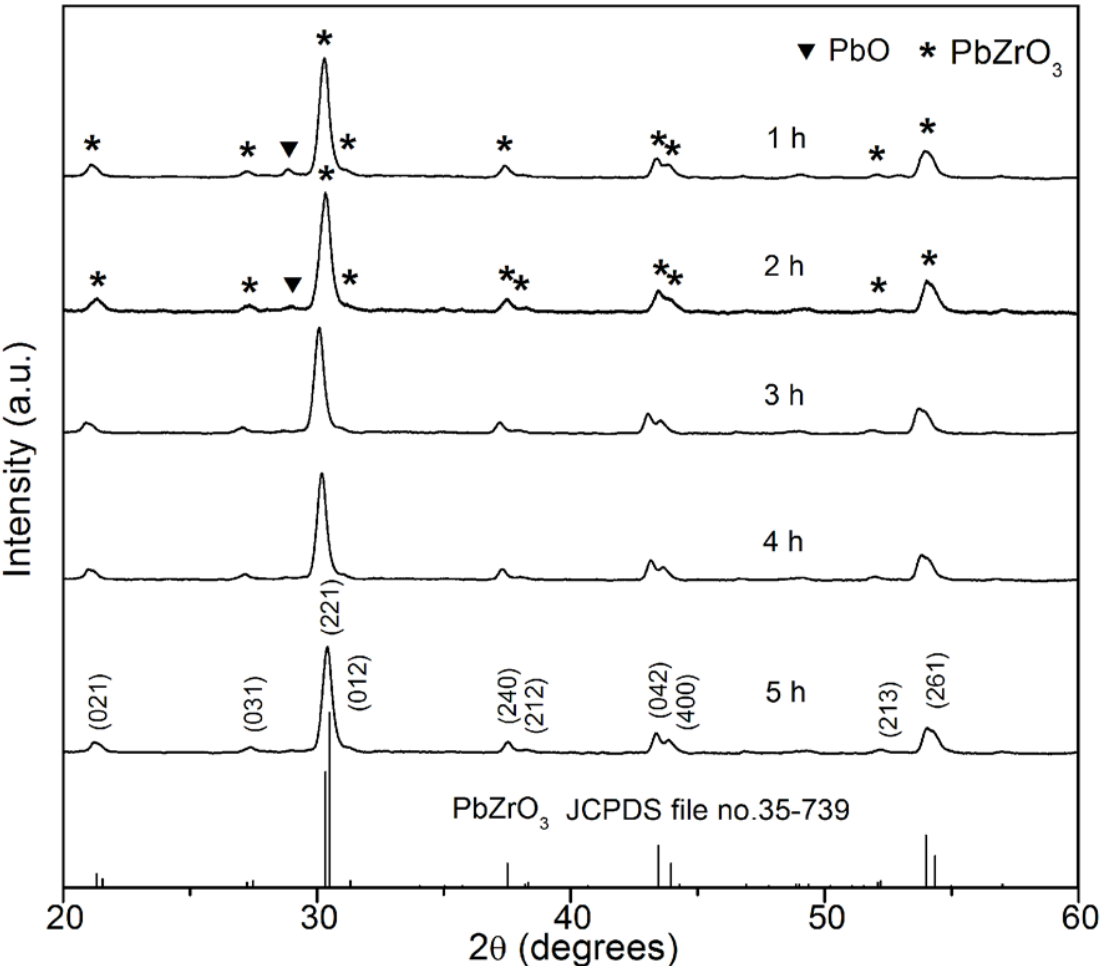
▼ PbO * $PbZrO_3$
1 h
2 h
3 h
4 h
5 h
Intensity (a.u.)
(021)
(031)
(221)
(012)
(240)
(212)
(042)
(400)
(213)
(261)
$PbZrO_3$ JCPDS file no.35-739
20
30
40
50
60
2θ (degrees)

Fig. 4

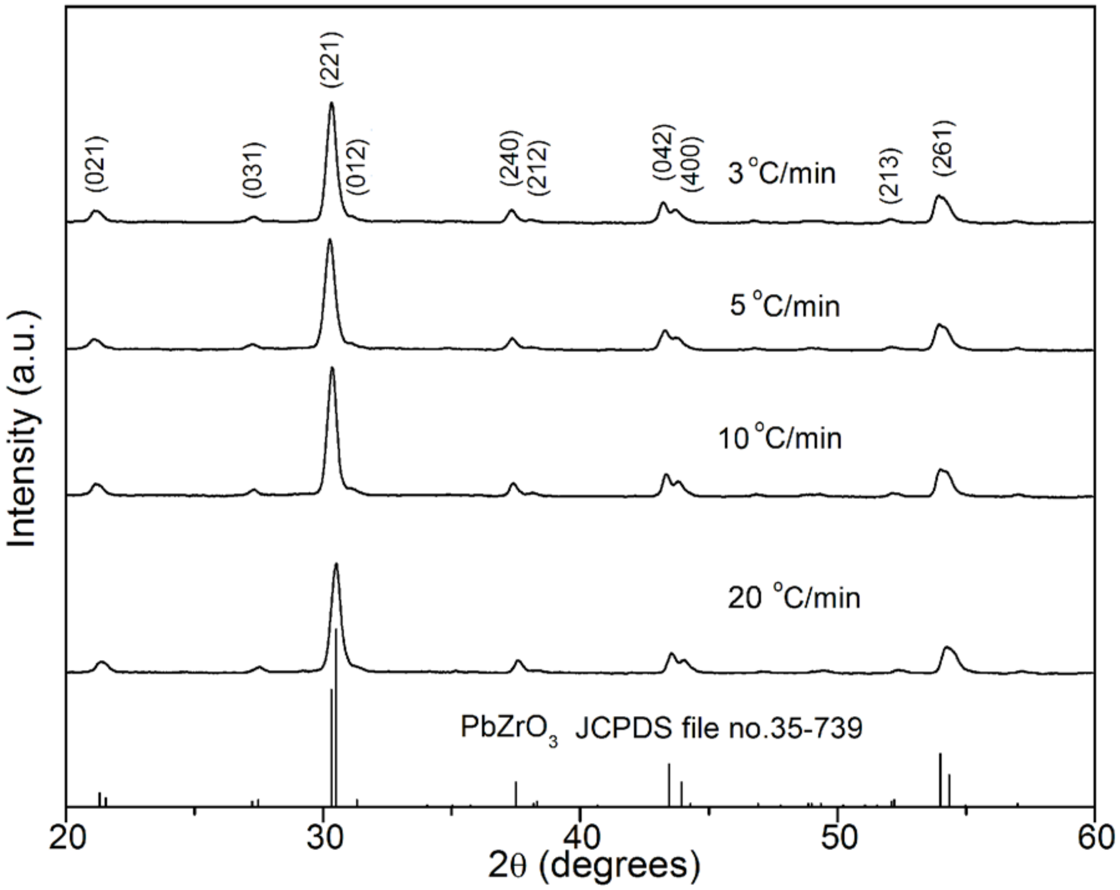
(021)
(031)
(221)
(012)
(240)
(212)
(042)
(400)
(213)
(261)
3 °C/min
5 °C/min
10 °C/min
20 °C/min
PbZrO$_3$ JCPDS file no.35-739
Intensity (a.u.)
20
30
40
50
60
2θ (degrees)

Fig. 5

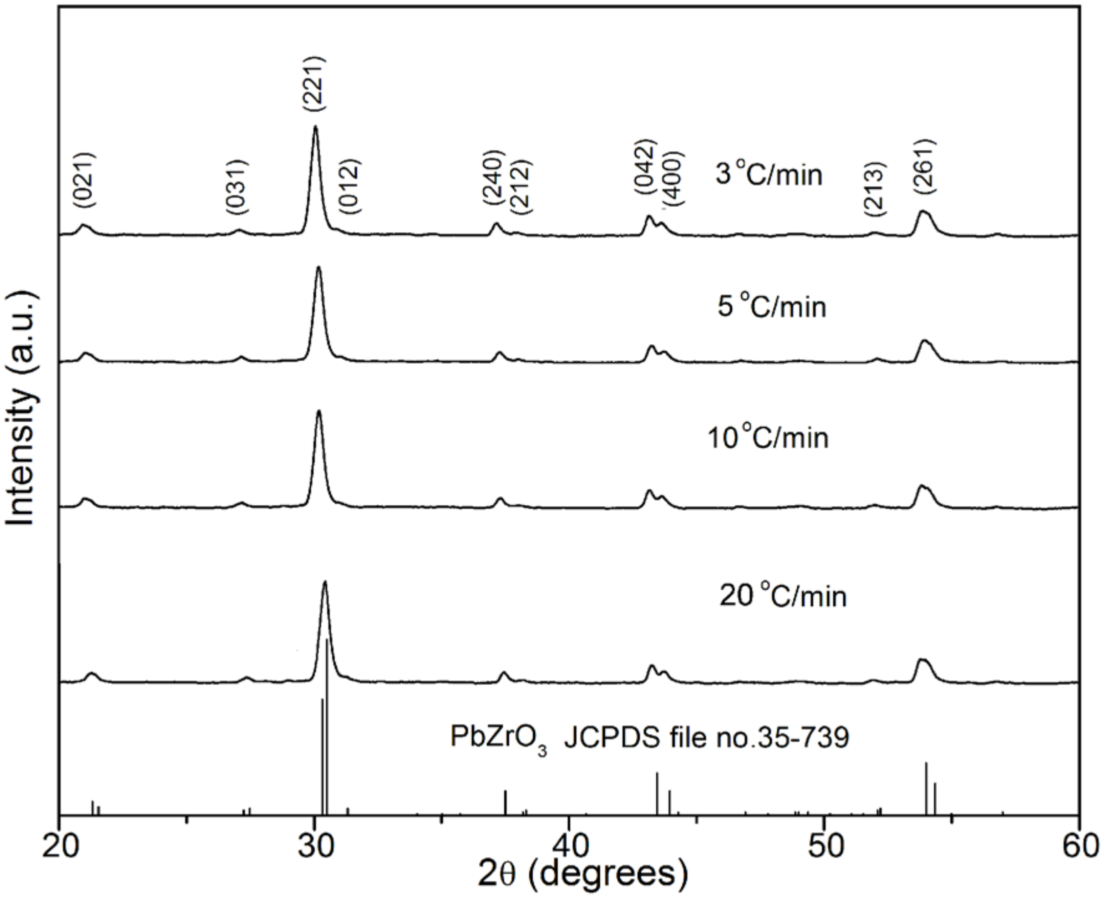
Intensity (a.u.)
2θ (degrees)
20
30
40
50
60
(021)
(031)
(221)
(012)
(240)
(212)
(042)
(400)
(213)
(261)
3 °C/min
5 °C/min
10 °C/min
20 °C/min
PbZrO3 JCPDS file no.35-739

Fig. 6

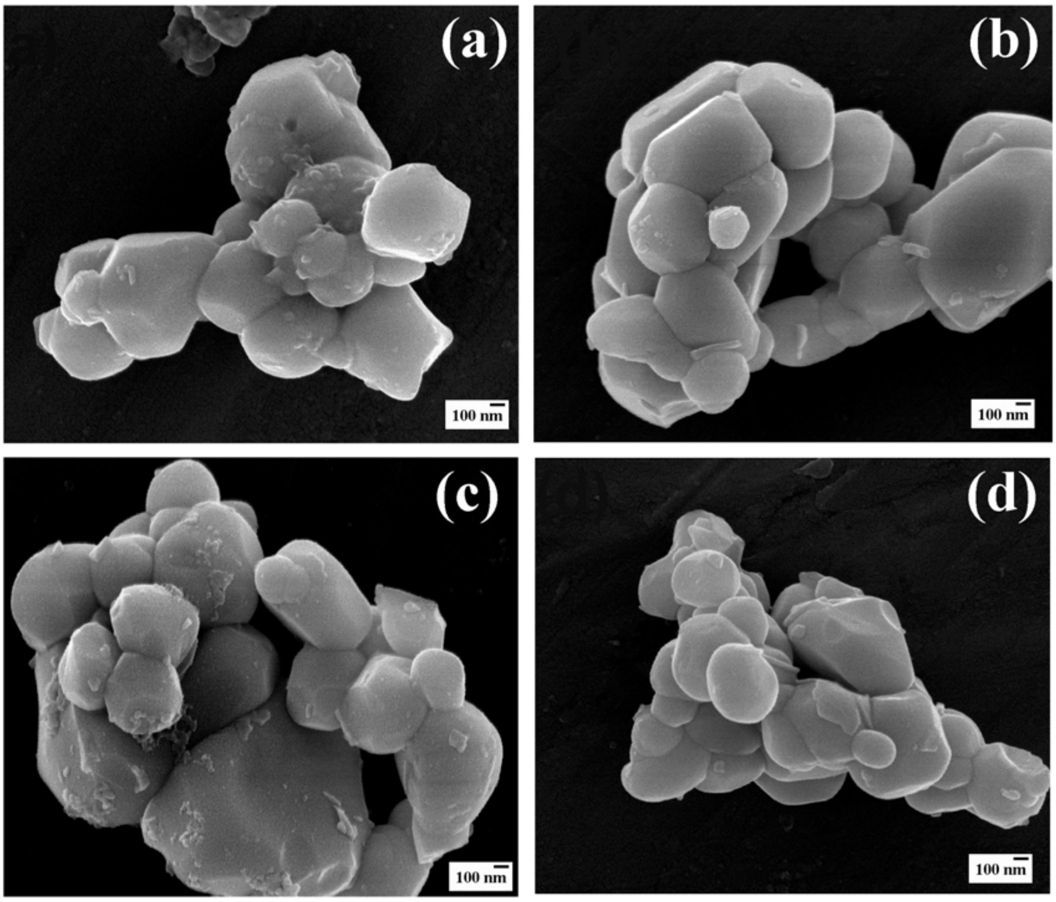

Fig. 7

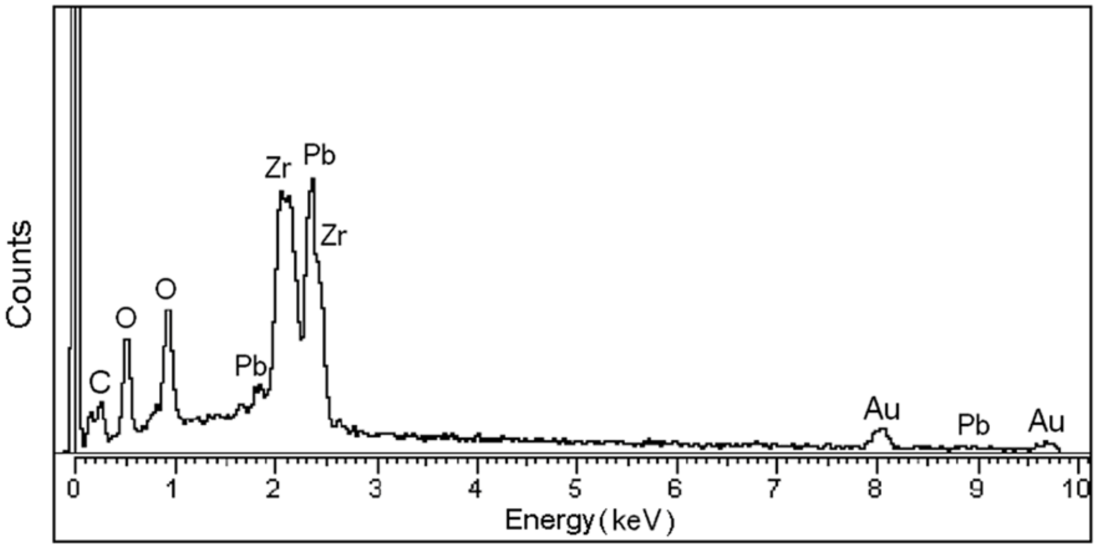

Fig. 8

Synthesis, Formation and Characterization of Lead Zinc Niobate – Lead Zirconate Titanate Powders via a Rapid Vibro-Milling Method

A. Ngamjarurojana*, O. Khamman, S. Ananta and R. Yimnirun

Department of Physics, Faculty of Science, Chiang Mai University,
Chiang Mai 50200, Thailand

***Corresponding author:** E-mail address: Ngamjarurojana@yahoo.com

ABSTRACT

In this study, an approach to synthesizing pyrochlore-free lead zinc niobate – lead zirconate titanate powders with a formula $x\mathrm{Pb}(\mathrm{Zn}_{1/3}\mathrm{Nb}_{2/3})\mathrm{O}_3$ $(1-x)\mathrm{Pb}(\mathrm{Zr}_{1/2}\mathrm{Ti}_{1/2})\mathrm{O}_3$ (when $x = 0.1\text{-}0.5$) by a mixed oxide synthetic route via a rapid vibro-milling has been developed. The formation of perovskite phase in calcined PZN-PZT powders has been investigated as a function of calcination temperature by TG-DTA and XRD techniques. Powder morphology and chemical composition have been determined with SEM and EDX techniques. The potential of a vibro-milling technique as a significant time-saving method to obtain single-phase PZN-PZT powders at low calcination temperature is also discussed. The results indicate that at calcination condition of 900 °C for 2h, with heating/cooling rates of 20 °C/min single-phase PZN-PZT powders can be obtained for every composition ratio between $x = 0.1\text{-}0.5$.

Keywords: Phase formation , Calcination ,Vibro-milling , Lead zinc niobate , Lead zirconate titanate

Introduction

Lead zirconate titanate, $Pb(Zr,Ti)O_3$ or PZT, is a well known piezoelectric that has been widely employed in a large number of sensing and actuating devices. PZT ceramics have very high Curie temperature (~ 390 °C). They have excellent dielectric, piezoelectric and elastic properties suitable for wide range of practical applications [1-3]. Lead zinc niobate, $Pb(Zn_{1/3}Nb_{2/3})O_3$ or PZN, which exhibits a perovskite structure and a Curie temperature ~ 140 °C, is one of the most important relaxor ferroelectric materials with high dielectric constant and large electrostrictive coefficient [4-5]. These characteristics make PZN a promising candidate for high performance electromechanical actuator and transducer applications. However, it has been recognized and widely accepted that inhomogeneous mixing in the conventional solid state reaction process leads to formation of pylochlore phase and subsequent deterioration of electrical properties in PZN ceramics [6-7]. The addition of other perovskite materials, such as barium titanate ($BaTiO_3$) [8], lead titanate ($PbTiO_3$) [9], or PZT [10], has been found to be effective in stabilizing PZN in the perovskite structure. However, recent work by Fan and Kim [11] has shown promise in producing only pure perovskite phase for PZN–PZT ceramics with the conventional mixed-oxide method.

The present work is aimed at synthesizing pyrochlore-free lead zinc niobate – lead zirconate titanate powders. The conventional mixed oxide synthetic route via a rapid vibro-milling has been developed with a one-step reaction of all starting materials. The rapid vibro-milling is employed for the first time in this work as a significant time-saving method to obtain single-phase PZN-PZT nano-sized powders at low temperature.

Experimental procedure

In this study, reagent grade oxides of lead oxide, PbO (Fluka Chemical, 99.9% purity), zirconium dioxide, ZrO_2 (RdH laborchemikalin, 99.9% purity), zinc oxide, ZnO (Fluka Chemical, 99.9% purity), niobium pentaoxide, Nb_2O_5 (Aldrich, 99.9% purity), and titanium dioxide, TiO_2 (RdH laborchemikalin, 99.9% purity), were used as the starting materials. PZN–PZT powders were synthesized by the solid-state reaction of these raw materials. Ground mixtures of the powders were required with stoichiometric ratios for the general composition $x\mathrm{Pb(Zn_{1/3}Nb_{2/3})O_3}$ $(1\text{-}x)\mathrm{Pb(Zr_{1/2}Ti_{1/2})O_3}$ where x = 0.1, 0.2, 0.3, 0.4, and 0.5. A McCrone vibro-milling technique was employed in order to combine mixing capacity with a significant time saving. The milling operation was carried out in isopropanol. High purity corundum cylindrical media were used as the milling media. After vibro-milling for 30 minutes and drying at 120 °C, the reaction of the uncalcined powders taking place during heat treatment was investigated by themogravimetric and differential thermal analysis (TG-DTA, Shimadzu) in air from room temperature up to 1350 °C. Based on the TG-DTA results, the mixture was calcined at temperatures between 750 to 950 °C for 2 hours in alumina crucible to examine the phase formation behavior of PZN-PZT powders. A heating/cooling rate of 20 °C/min was selected for all of the compositions in this system because it was shown to be effective in reducing the total amount of pyrochlore phase [12].

Calcined powders were subsequently examined by room temperature X-ray diffraction (XRD; Siemens-D500 diffractrometer) using Ni-filtered CuK radiation to identify the phases formed for the PZN-PZT powders. The relative amounts of perovskite and pyrochlore phases were approximated by calculating the ratio of the major XRD peak intensities of the perovskite and pyrochlore phases via the following equation:

$$\text{Perovskite \%} = \frac{I_{perov}}{I_{perov} \quad I_{pyro}} \quad 100$$

where I_{perov} and I_{pyro}, refer to the intensity of the (110) perovskite peak and (222) pyrochlore peak, respectively. Powder morphologies and particle sizes were directly imaged using scanning electron microscopy (SEM; JEOL JSM-840A). EDX spectra were quantified with the virtual standards peaks supplied with the Oxford Instruments eXL software. Diagram of experimental procedure is shown in Fig. 1.

Results and Discussion

Themogravimetric and Differential Thermal Analysis (TG/DTA)

TG-DTA curves obtained for powders mixed in the stoichiometric proportions of PZN and PZT powders are displayed in Fig. 2. In the temperature range 50 – 300 ^{o}C, the sample shows several large exothermic peaks in the DTA curve. These DTA peaks can be attributed to the decomposition of the organic species from the milling process. The different temperatures, intensities, and shapes of the thermal peaks are probably related to the different natures of the organic species and, consequently, caused by the removal of differently bounded species in the network [13]. In the temperature range 750^{o} – 1050 ^{o}C, both exothermic and endothermic peaks are observed in the DTA curve. The enlarge zone of this DTA curve shows that the endothermic peak centered at ~ 800 ^{o}C may result from perovskite phase crystallization, and the last exothermic peak centered at ~ 850 ^{o}C may be caused by the decomposition of lead oxide [14,15]. Above 1000 ^{o}C, TG curve indicates that higher weight loss of substance occurs. This TG result implies the upper limit of the calcination temperature for the mixed powders. Therefore, these temperatures are used to define the ranges of calcination temperatures (750 to 950 ^{o}C) used in subsequent powder processing steps.

X-Ray Diffraction Analysis (XRD)

Powder XRD patterns of the calcined *0.5*PZN-*0.5*PZT powders at different calcination temperatures are shown in Fig. 3. The XRD results show that the pyrochlore phase $Pb_{1.88}(Zn_{0.3}Nb_{1.25})O_{5.305}$ (JCPDS No.25-0446) is dominant at the calcination temperature below 850 C for the powders. The precursor phases of PbO, ZnO, Nb_2O_5, ZrO_2, TiO_2 are also detected in the powders by XRD when calcined below 800 ^{o}C. Other compositions also show a similar trend. The pyrochlore-free xPZN (1-x)PZT powders with x= 0.1- 0.4 can be obtained at calcination temperatures above 850 C. Earlier study by Vittayakorn *et. al.* [16] showed similar observation. However, in that study which used a conventional ball-milling method with excess PbO 2wt% the calcination temperature was above 900 ^{o}C. This clearly indicates that a rapid vibro-milling method can lower the calcination temperature for PZN-PZT powders.

As listed in Table I, all the compositions in the present work exhibit pyrochlore-free XRD scans at calcination temperature of 900 C. It can be noticed that in most compositions the perovskite phase is formed in a sudden nature, which is significantly different from previous research [16] in which more perovskite phase was found with increasing calcination temperature. The difference could be attributed to the nano-sized mixed powders (50-300 nm) obtained from a rapid vibro-milling technique. The perovskite phase formation behavior for xPZN *(1-x)*PZT powders at the calcination temperature of 900 C is shown in Fig. 4. The percentage of perovskite phase in PZN-PZT powders is summarized in Table I as a function of calcination temperature. These experimental results indicate that when the concentration of the PZN phase increases the calcination temperature must be increased to obtain single perovskite phase of PZN-PZT powders. Even though pyrochlore-free PZN-PZT powders can be obtained at calcination temperature of 900 C for all compositions (*x* = 0.1-0.5), it should be noted that the on-set calcination temperature for pyrochlore-free powders starts at 800 C for composition with *x* = 0.1. It is also very interesting to see that the on-set temperature in every composition is approximately 50 C lower that those reported earlier with the conventional ball-milling method [16]. More importantly, this study suggests that the conventional mixed oxide method helps to stabilize the perovskite phase and the calcination temperature can be lowered by a vibro-milling technique.

SEM and EDX Analysis

The morphological changes in the PZN-PZT powders formed by a mixed oxide method are illustrated in Fig. 5. In general, the particles are agglomerated and basically irregular in shape, with a substantial variation in particle size, particularly in samples with more PZN contents. Generally, particle size of all compositions can be estimated from SEM micrographs to be in range of 0.2-2 m. It should be noted that the morphology of the calcined 0.1PZN-0.9PZT and 0.3PZN-0.7PZT powders is almost similar in size and shape, while for the other compositions the size and shape of the powders are significantly different.

Finally, EDX analysis using a 20 nm probe on a large number of particles of the calcined powders confirms that the parent composition is PZN-PZT powders, in good agreement with XRD results.

Conclusions

The solid-state mixed oxide method via a vibro-milling technique is explored in the preparation of pyrochlore-free solid solution of xPZN-(1-x)PZT powders (when x= 0.1-0.5). The optimum calcination condition for the formation of perovskite phase PZN-PZT powders is found to be 900 ^{o}C for 2 h with heating/cooling rates of 20 ^{o}C / min. Clearly, XRD study indicates that phase pure perovskite PZN-PZT powders have been obtained in this study. The potential of a vibro-milling technique as a significant time-saving method to obtain single-phase PZN-PZT powders at lower calcination temperature has also been demonstrated.

Acknowledgements

The authors are grateful to the Thailand Research Fund (TRF), Graduate School and Faculty of Science, Chiang Mai University, and Ministry of University Affairs of Thailand for financial support.

References

[1] Jaffe, B., Cook Jr., W. R. and Jaffe, H., *Piezoelectric Ceramics*. Academic Press, London, UK, 1971.

[2] Xu, Y., *Ferroelectric Materials and Their Applications*. Elsevier Science, Amsterdam, The Netherlands, 1991.

[3] Haertling, G. H., *J.Am. Ceram. Soc.*, 1999, **82**, 797–818.

[4] Kuwata, J., Uchino, K. and Nomura, S., *Ferroelectrics*, 1979, **22**, 863–867.

[5] Park, S. E. and Shrout, T. R., *J. Appl. Phys.*, 1997, **82**, 1804–1811.

[6] Dambekalne, M., Brante I. and Sternberg,A., *Ferroelectrics*, 1989, **90**,1-14.

[7] Shrout, T. R. and Halliyal, A., *Am. Ceram. Soc. Bull.*, 1987, **66**, 704–711.

[8] Halliyal, A., Kumar, U., Newnham, R. E. and Cross, L. E., *Am. Ceram. Soc. Bull.*, 1987, **66**, 671–676.

[9] Gururaja, T. R., Safari, A. and Halliyal, A., *Am. Ceram. Soc. Bull.*, 1986, **65**, 1601–1603.

[10] Fan, H.and Kim, H. E., *J. Appl. Phys.*, 2002, **91**, 317–322.

[11] Fan, H. and Kim, H. E.,, *J. Mater. Res.,* 2002, **17,** 180-185.

[12] Vittayakorn, N., Rujijanagul G., Tunkasiri T., Tan X., Cann D.P., *J. Mater. Res.*, 2003, **18**, 2882–2889.

[13] Ananta, S., Brydson, R., Thomas, N.W., *J. Eur. Ceram. Soc.*, 2000, **20**, 2325-2329.

[14] Tien, T.Y., Carlson, W.G*., J. Am. Ceram. Soc.*,1962, **45**, 567-571.

[15] Pillai, C.G., Ravindran, P.V., *Thermochim. Acta.,* 1996, **278,** 109-118.

[16] Vittayakorn, N., Rujijanagul G., Tunkasiri T., Tan X., Cann D.P., *J. Mater. Sci. and Eng. B.*, 2004 **, 108,** 258–265.

Table I. Percentage of perovskite phase of (*1*-*x*)PZT-*x*PZN; *x* = *0.1*-*0.5*.

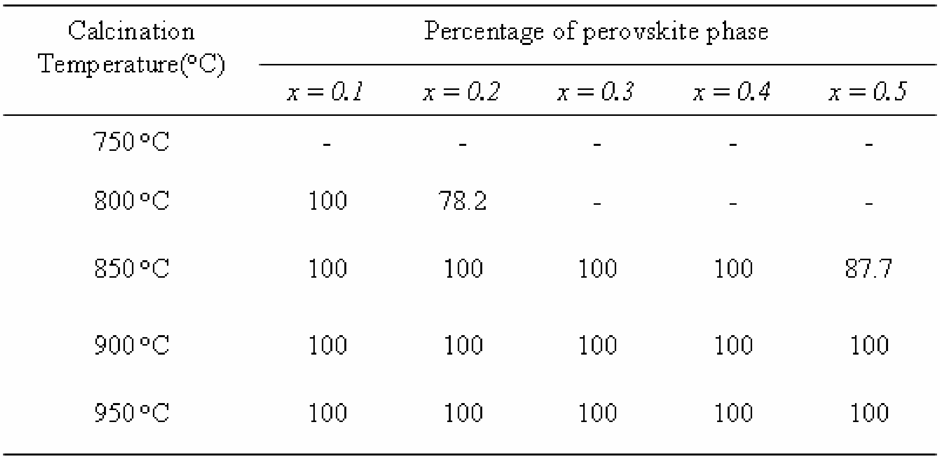

Calcination Temperature(°C)	Percentage of perovskite phase				
	$x = 0.1$	$x = 0.2$	$x = 0.3$	$x = 0.4$	$x = 0.5$
750 °C	-	-	-	-	-
800 °C	100	78.2	-	-	-
850 °C	100	100	100	100	87.7
900 °C	100	100	100	100	100
950 °C	100	100	100	100	100

List of Figure Captions

Figure 1 Diagram of experimental procedure.

Figure 2 TG-DTA curves for the mixture of PZN-PZT powder after vibro-milling.

Figure 3 XRD patterns of 0.5PZN–0.5PZT powder calcined at various temperatures temperature for 2 h. with heating/cooling rates of 20 °C / min.

Figure 4 XRD patterns of the *x*PZN - (1-*x*)PZT powders (when $x = 0.1, 0.2, 0.3, 0.4$, and 0.5) calcined at 900 °C with heating/cooling rates of 20 °C/min and soaking time of 2 h.

Figure 5 SEM micrographs of the *x*PZN - (1-*x*)PZT powders calcined at 900 °C with heating/cooling rates of 20 °C/min and soaking time of 2 h for (a) x=0.1, (b) x=0.2, (c) x=0.3, (d) x=0.4 and (e) x=0.5.

Figure 1

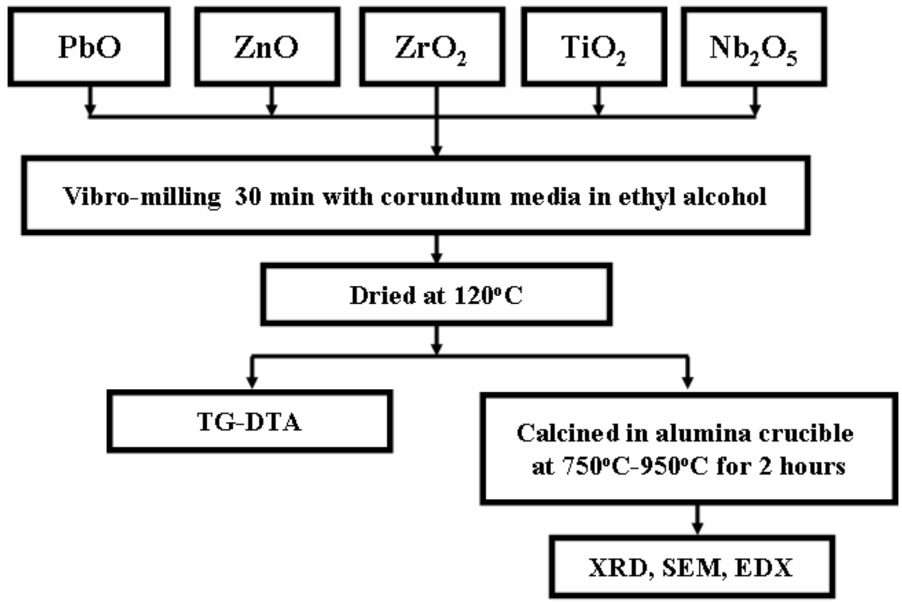
PbO
ZnO
ZrO₂
TiO₂
Nb₂O₅
Vibro-milling 30 min with corundum media in ethyl alcohol
Dried at 120°C
TG-DTA
Calcined in alumina crucible at 750°C-950°C for 2 hours
XRD, SEM, EDX

Figure 2

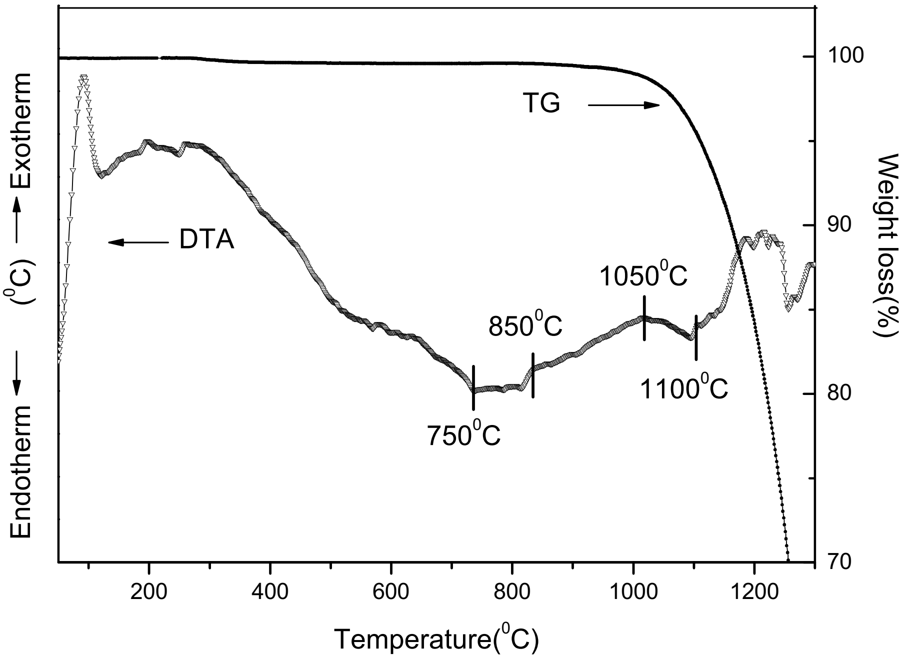
Endotherm ⟵ (⁰C) ⟶ Exotherm
Weight loss(%)
Temperature(⁰C)
TG
DTA
750⁰C
850⁰C
1050⁰C
1100⁰C
200
400
600
800
1000
1200
100
90
80
70

Figure 3

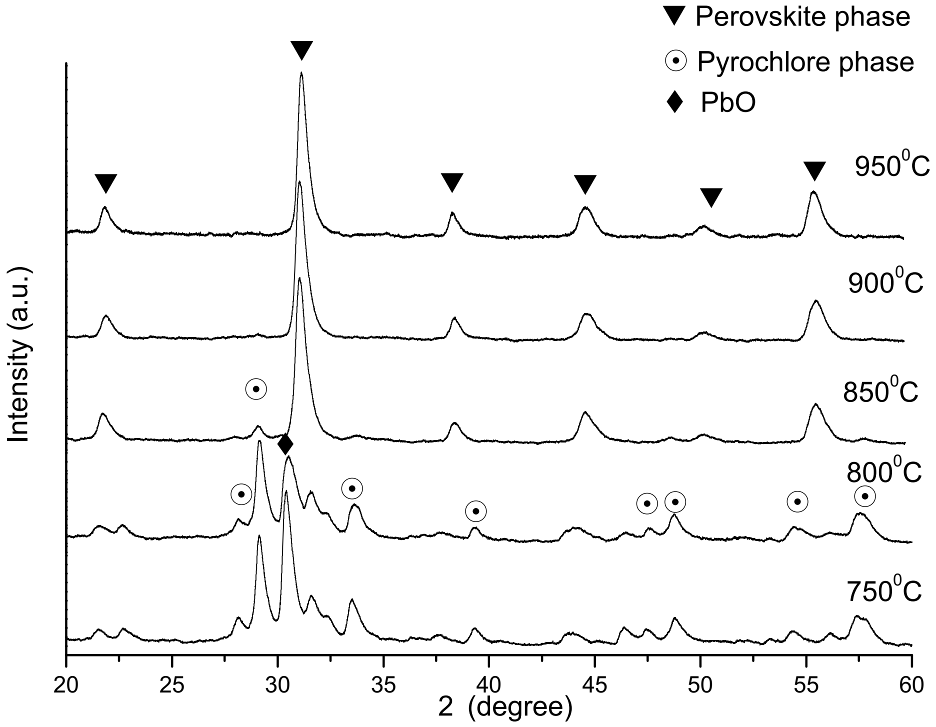
▼ Perovskite phase
⊙ Pyrochlore phase
♦ PbO
950^{0}C
900^{0}C
850^{0}C
800^{0}C
750^{0}C
Intensity (a.u.)
2 (degree)
20
25
30
35
40
45
50
55
60

Figure 4

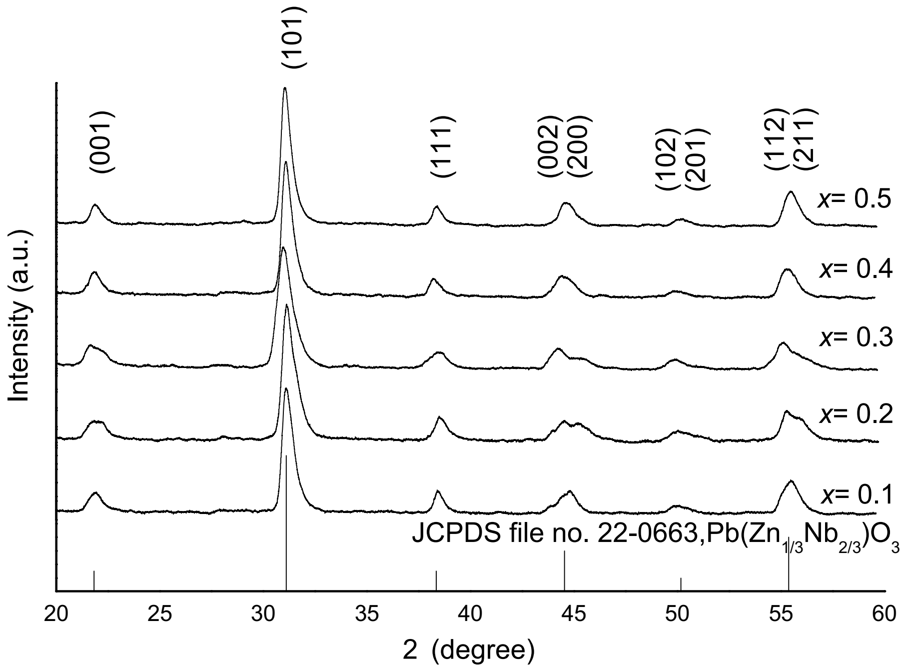
(001)
(101)
(111)
(002)
(200)
(102)
(201)
(112)
(211)
x= 0.5
x= 0.4
x= 0.3
x= 0.2
x= 0.1
JCPDS file no. 22-0663,Pb(Zn$_{1/3}$Nb$_{2/3}$)O$_3$
Intensity (a.u.)
20
25
30
35
40
45
50
55
60
2 (degree)

Figure 5

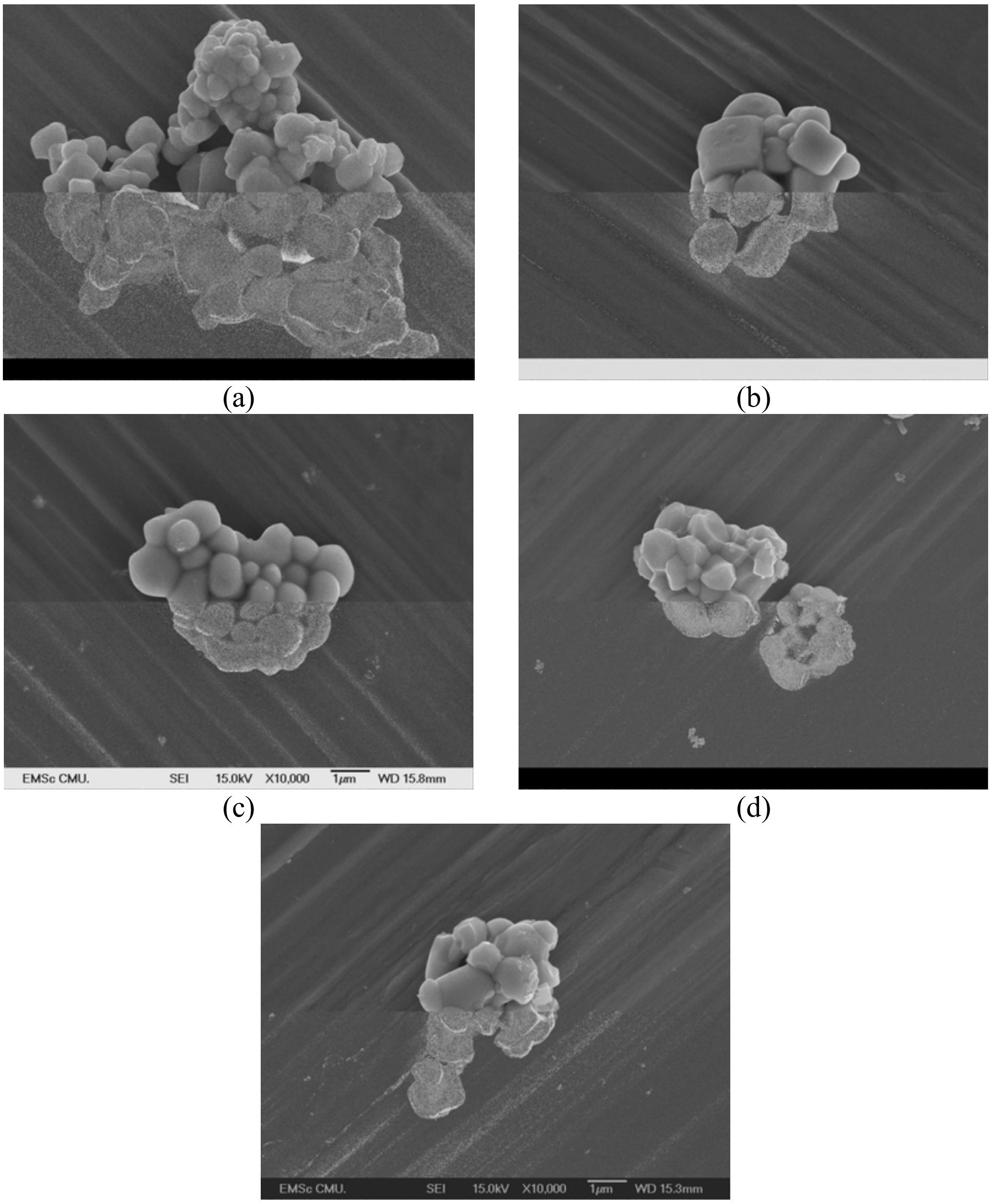

(a) (b) (c) (d) (e)

Synthesis, Formation and Characterization of Lead Indium Niobate-Lead Titanate Powders

S. Wongsaenmai, O. Khamman, S. Ananta and R. Yimnirun
Department of Physics, Faculty of Science, Chiang Mai University,
Chiang Mai 50200, Thailand
Correspondence Author E-mail: wongsaenmai@yahoo.com

Abstract

In this study, powders of lead indium niobate-lead titanate $(1-x)Pb(In_{1/2}Nb_{1/2})O_3-(x)PbTiO_3$ (PINT) binary system near the morphotropic phase boundary (MPB) composition with x = 38mol% PT are synthesized with the conventional mixed oxide and the wolframite methods via a rapid vibro-milling technique for the first time. The preparation method and calcination temperature have been found to show pronounced effects on the phase formation behavior of the PINT powders. The stabilized perovskite phase form of PINT can be synthesized by the wolframite method, while precursor phases are still found in powders prepared by the conventional method. Finally, this study shows that the rapid vibro-milling mixing technique is effective in preparing the phase pure perovskite of PINT powders.

Keywords: PIN-PT, Conventional mixed oxide, Wolframite method, vibro-milling technique

Introduction

Lead indium niobate $Pb(In_{1/2}Nb_{1/2})O_3$ (PIN) compounds are interesting for studying the kinetics of compositional ordering [1]. It has been reported that the degrees of ordering on the B-site can be varied by thermal annealing and by forming solid solutions with perovskite compounds that exhibit normal dielectric behavior, such as $Pb(Fe_{1/2}Nb_{1/2})O_3$ (PFN), $PbZrO_3$ (PZ) and $PbTiO_3$ (PT) [2]. With different thermal treatments, the degrees of the In/Nb cation ordering on the B-site in a perovskite structure can be manipulated from a structurally disordered state into various degrees of ordering. The disorder PIN is a relaxor ferroelectric with a psudo-cubic perovskite structure. It shows the relaxor behavior with a broad dielectric maximum near 66°C, when measured at 1 kHz [3,4]. On the other hand, the ordered PIN has the antiferroelectric orthorhombic phase [5-9] with a sharp peak in the dielectric constant at 168°C [4,10]. However, pure-phase perovskite PIN ceramics free of the pyrochlore phase are very difficult to prepare using a conventional mixed oxide methode [7, 11]. This is because the tolerance and the electronegativity difference of PIN are very low compared with other perovskite compounds such as PMN [2, 12]. The wolframite method, as used by Groves [13] for the preparation of perovskite PIN ceramic, is not effective in suppressing pyrochlore phase formation. The addition of excess In_2O_3 was shown to yield higher amount of perovskite phase [13]. Recently, Alberta and Bhalla [7] were able to produce 100% phase-pure perovskite PIN ceramic with the addition of excess indium and/or lithium with wolframite method. Moreover, the solid solution with perovskite compounds such as $PbTiO_3$, can stabilize the perovskite phase of PIN and chemical ordering may be suppressed. It has also been reported that a morphotropic phase boundary of the solid solution system $(1-x)Pb(In_{1/2}Nb_{1/2})O_3-(x)PbTiO_3$ is located at a composition with x=0.38 [14, 15] and this binary system near MPB composition belongs to one of the relaxor-PT systems with T_c higher than 250°C [16, 17]. Previous studies have focused on the properties of solid solution PIN-PT single crystals, while the information on PIN-PT ceramics is still limited.

This study is intended to explore a synthetics route for the pure-phase perovskite bodies of PINT binary system near MPB composition. Both the conventional mixed-oxide and the wolframite methods have been employed. More importantly, a rapid vibro-milling mixing technique is utilized to obtain phase-pure perovskite powders. Finally, the phase formation and morphology of the powders calcined at various temperatures are studied.

Experimental

For the conventional method, the starting materials of lead oxide, PbO (Fluka, 99% purity), titanium oxide, TiO_2 (Riedel-de Haën, 99% purity), niobium oxide, Nb_2O_5 (Aldrich, 99.9% purity) and indium oxide, In_2O_3 (Aldrich, 99.99% purity) were mixed in the required stoichiometric ratio for the composition $(1-x)Pb(In_{1/2}Nb_{1/2})O-(x)PbTiO_3$ where $x = 0.38$. The oxide powders were milled via a rapid vibro-milling technique for 30 min with corundum media in ethanol [18]. After drying at 120°C, the mixture was calcined at temperature between 700 to 1000 °C with dwell time of 2 h and heating/cooling rate of 10°C /min in a double crucible [19]. On the other hand, in the wolframite method the wolframite precursor was first prepared from oxide powders of niobium oxide, (Nb_2O_5) and indium oxide, (In_2O_3). The intermediate precursor $InNbO_4$ was synthesized at an optimized calcination temperature of 1100°C for 2 h [20]. The wolframite precursor was then mixed with lead oxide (PbO) and titanium oxide (TiO_2) and re-milled. After drying, the mixture was calcined at temperature between 700 to 1000 °C with dwell time of 2 h and heating/cooling rate of 10°C/min in a double crucible.

In order to study the reaction of the uncalcined PINT powders, a differential thermal analysis (DTA) and thermalgravity analysis (TG) were performed on a DTA-TG apparatus (Perkin Elmer) using heating/cooling rate of 10°C/min in air from room temperature up to 1300°C. X-ray diffraction (XRD; Siemen-D500 diffractometer) was used to determine the phase formation behavior of the calcined powders. The microstructure was observed with a scanning electron microscope (SEM; Joel JSM-840A). The chemical compositions of the phase formed were elucidated by an energy-dispersive X-ray (EDX) analyzer with an ultra-thin window.

Results and Discussion

Initially, the DTA-TG analysis was performed on uncalcined powders to obtain thermal behavior to define the range of calcination temperature for the XRD investigation. The results from DTA-TG studies indicate that the suitable range of the calcination temperature is between 700 and 1000 °C.

Fig. 1 shows the XRD patterns of powders calcined for 2 h between 700°C and 1000°C with heating/cooling rate of 10°C/min. The differences in XRD patterns for both methods are clearly apparent. The calcination temperature of 700°C does not yield the perovskite phase for both methods. At 850℃ and 800°C, respectively, the perovskite phase is found to form for the conventional and wolframite methods. The optimum calcination temperature for the formation of phase pure perovskite PINT is found to be about 900°C for the wolframite method, while the conventional method is found to be about 850°C with PT peak. The experiment indicates that the wolframite method helps to stabilize the perovskite phase in PINT system. More importantly, though the conventional method yields the perovskite phase at lower temperature than the wolframite method, the strong PT peak is still observed in the XRD patterns of powders calcined with the conventional method as high as 1000 °C (as seen in Fig. 1a). Clearly, the significant difference between the XRD patterns is the presence of the strong PT peak at 31.5° for the powders calcined with the conventional method. As seen in Fig. 2, the diffraction peak does not match any peaks of $Pb(In_{1/2}Nb_{1/2})O_3$ (PIN) and $PbTiO_3$ (PT) compounds. Instead, the peaks closely match to those of a hypothetical solid solution formed between the two compounds. Furthermore, for the wolframite method the peaks are not a simple superposition corresponding to the two compounds, while the corresponding diffraction angle at 31.5° can be matched to maximum peak of PT for the conventional method [21]. This observation points to the formation of PT phase in the powders from the conventional method, which could be a result of better reaction of PbO and TiO_2 to form PT phase rather than PINT phase. As listed in Table 1, the quantitative analysis by energy dispersive X-ray (EDX) shows that, in addition to the PINT phase, the PIN, PT and TiO_2 phases are also present in the powders calcined by the conventional method, while only additional Nb_2O_5 phase (undetected by XRD) is possible in the powders obtained from the wolframite method. A combination of the XRD and EDX methods has indicated that the wolframite method yields XRD-phase pure PINT powders, while the conventional one results in a mixture of PINT, PIN PT, and TiO_2 (undetected by XRD) phases. This clearly emphasizes the importance of the synthetic route used to prepare the PINT powders. Moreover, effects of soaking time and heating/cooling rates have also been studied in this work. For this study, it is found that the soaking time and heating/cooling rate do not significantly affect the phase formation behavior of PINT powders.

The morphological evolution of the calcined powders was investigated by scanning electron microscopy (SEM). Fig. 3 shows the SEM micrographs of the powders synthesized by conventional and wolframite methods. In general, the particles are agglomerated and irregular in shape. As seen in Fig. 3a, the particles synthesized by the conventional method show relatively large agglomerates ranging in diameter from about 0.5 to 2 μm. On the other hand, the particles synthesized by wolframite method, with diameter in the range ~ 0.1 to 1 μm (Fig. 3b), are lower in particle agglomeration than the conventional method.

Conclusions

The powders of a solid solution of $(1-x)Pb(In_{1/2}Nb_{1/2})O_3-(x)PbTiO_3$ binary system with x=0.38 was successfully prepared by both the conventional mixed oxide and the wolframite methods. The results from DTA-TG technique were use used to define the range of calcination temperature with 700°C to 1000°C. The optimum calcination temperature for the formation of phase pure perovskite was determined to be 900°C and 850°C for the wolframite, and the conventional methods, respectively, with soaking time of 2 h and heating/cooling rate of 10°C/min. Moreover, the perovskite phase was found to form at lower temperature with the conventional method than the wolframite method. However, the EDX studies showed that the stabilized perovskite phase form of PINT can be synthesized by the wolframite method, while precursor phases were still found in powders prepared by the conventional method. Moreover, the large agglomeration and particles size were observed in powder synthesized by the conventional method.

Acknowledgement

The authors would like to express their gratitude for financial support from the Thailand Research Fund (TRF) and Graduate School and Faculty of Science, Chiang Mai University, and Ministry of University Affairs of Thailand.

.

References

[1]. A.A. Bokov, I.P. Rayevskii, V.G. Smotrakov and O.I. Prokopalo, *Phys. Stat. Sol. (a)*, **93**, 411-417 (1986).

[2]. T.R. Shrout and A. Halliyal, *Am. Ceram. Soc. Bull.*, **66(4),** 704-711 (1987).

[3]. E.F. Alberta and A.S. Bhalla, *Mater. Lett.*, **40**, 114-117 (1999).

[4]. E.F. Alberta and A.S. Bhalla, *J. Phys. Chem. Solids.*, **63**, 1759-1769 (2002).

[5]. C.A. Randall, D.J. Barber, P. Groves and R.W. Whatmore, *J. Mater. Sci.*, **23**, 3678-3682 (1988).

[6]. N. Yasuda and T. Mizuno, *Appl. Phys. Lett.*, **66(5)**, 571-573 (1995).

[7]. E.F. Alberta and A.S. Bhalla, *Mater. Lett.*, **29**, 127-129 (1996).

[8]. E.F. Alberta and A.S. Bhalla, *Ferroelectrics*, **188**, 96-107 (1996).

[9]. N. Yasuda, H. Ohwa, T. Mizunao, M. Iwata and Y. Ishibashi, *Appl. Phys. Lett.,* **68(24),** 3404-3406 (1996).

[10]. M. Iwata, S. Katagiri, H. Orihara, M. Maeda, I. Zusuki, H. Ohwa, N. Yasuda and Y. Ishibashi, *Ferroelectrics.*, **301**, 179-183 (2004).

[11]. Y. Yoshikawa, *J. Eur. Ceram. Soc.,* **21**, 2041-2045 (2001).

[12]. Y. Guo, H. Luo, T. He and Z. Yin, *Solid. State. Commun.*, **123**, 417-420 (2002).

[13]. P. Groves, *Ferroelectrics*, **65**, 67-77 (1985).

[14]. E.F. Alberta and A.S. Bhalla, *J. Koren. Phys. Soc.*, **32**, S1265-S1267 (1998).

[15]. N. Yasuda, H. Ohwa, D. Hasegawa, H. Hosono, Y. Yamashita, M. Iwata and Y. Ishibashi, *Ferroelectrics*, **270**, 247-252 (2002).

[16]. N. Yasuda, H. Ohwa, M. Kume and Y. Yamashita, *J. Appl. Phys.*, **39(2A),** L66-L68 (2000).

[17]. N. Yasuda, H. Ohwa, M. Kume, K. Hayashi, Y. Hosono and Y. Yamashita, *J. Cryst. Growth,* **229**, 299-304 (2001).

[18]. R. Tipakontitikul and S. Ananta, *Mater. Lett.,* **58(3),** 449-454 (2004).

[19]. N. Vittayakorn, G. Rujijanagul, T. Tunkasiri, X. Tan and D.P. Cann, *Mat. Sci. Eng. B-Solid.,* **108**, 258-265 (2004).

[20]. N. Yasuda and M. Fujie, Jnp. J. Appl. Phys., 31, 3128-3131, (1992).

[21]. N. Yasuda, H. Ohwa, M. Kume, K. Hayashi, H. Hosono and Y. Yamashita, *J. Cryst. Growth*, **229**, 299-304 (2001).

List of Table Caption

Table 1 Chemical compositions of calcined powders from SEM-EDX analysis

List of Figure Captions

Table 1 Chemical compositions of calcined powders from SEM-EDX analysis

Method	Composition (at.%)				Possible Phases
	Pb (M)	In (L)	Nb (L)	Ti (K)	
Conventional	43.9	11.3	14.4	30.4	$PbIn_{0.31}Nb_{0.31}Ti_{0.38}O_3$, $Pb(In_{1/2}Nb_{1/2})O_3$, $PbTiO_3$, TiO_2
Wolframite	46.6	11.9	21.0	20.5	$PbIn_{0.31}Nb_{0.31}Ti_{0.38}O_3$, Nb_2O_5

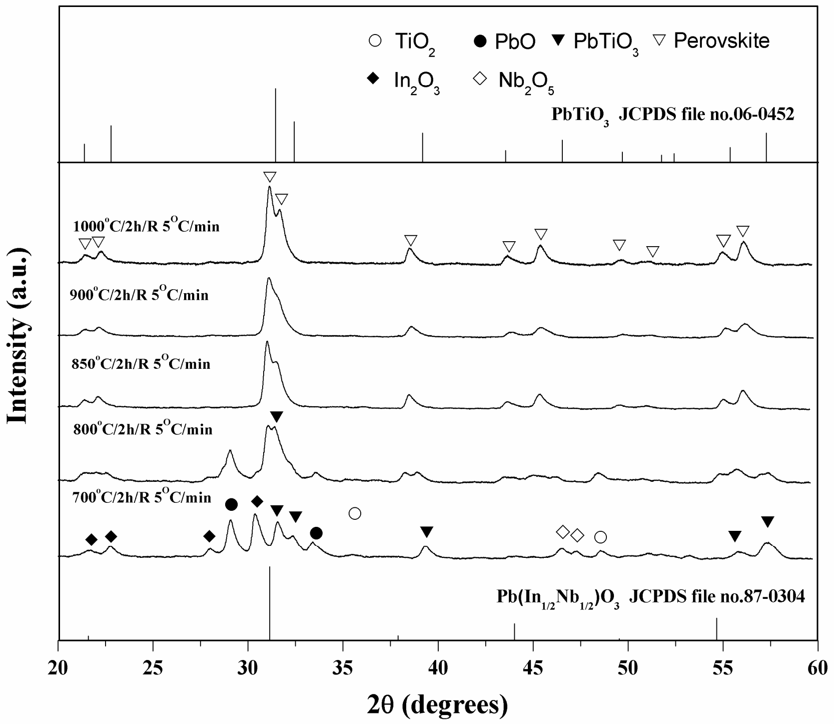

(a)

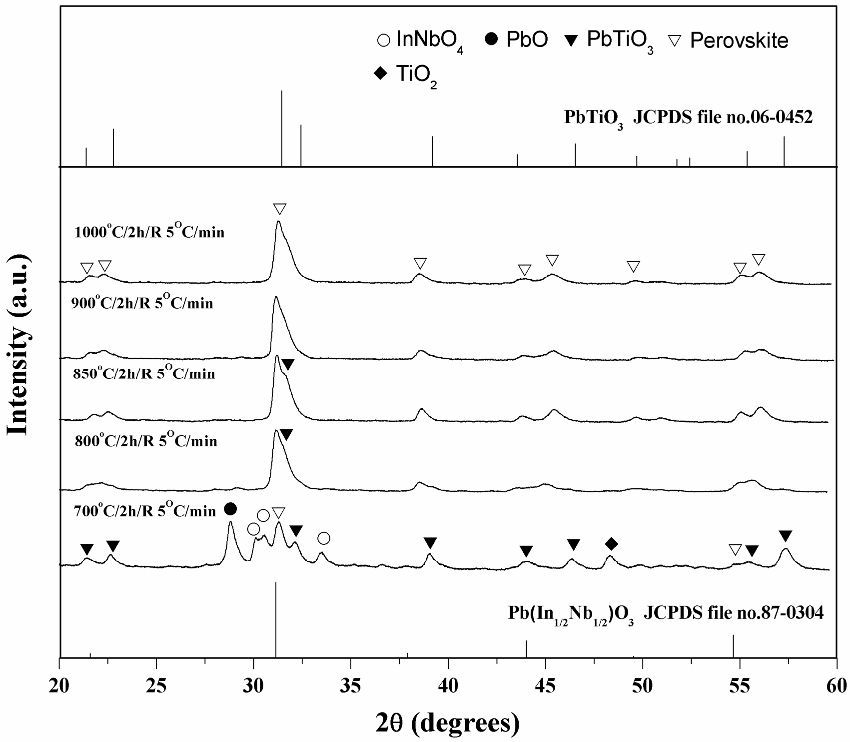

(b)

Fig.1 XRD patterns as a function of the calcination temperature for (a) the conventional method and (b) the wolframite method

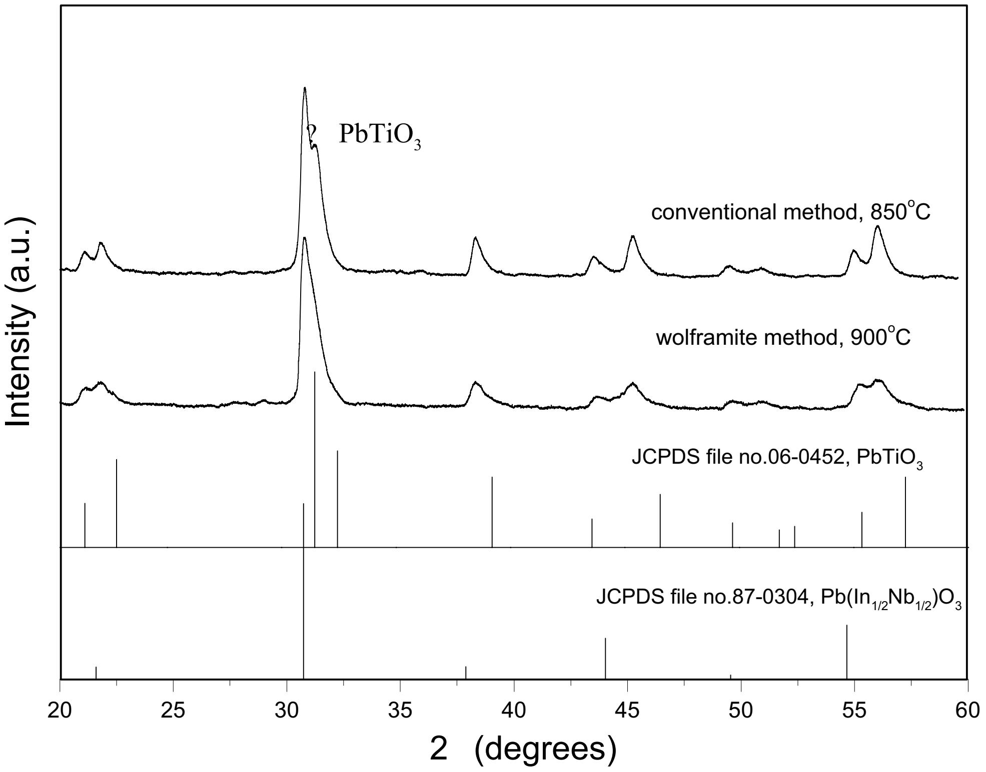

Fig. 2 XRD patterns for PINT powders at optimum calcination temperature of both methods, with comparison to standard JCPDS files for PIN and PT compounds

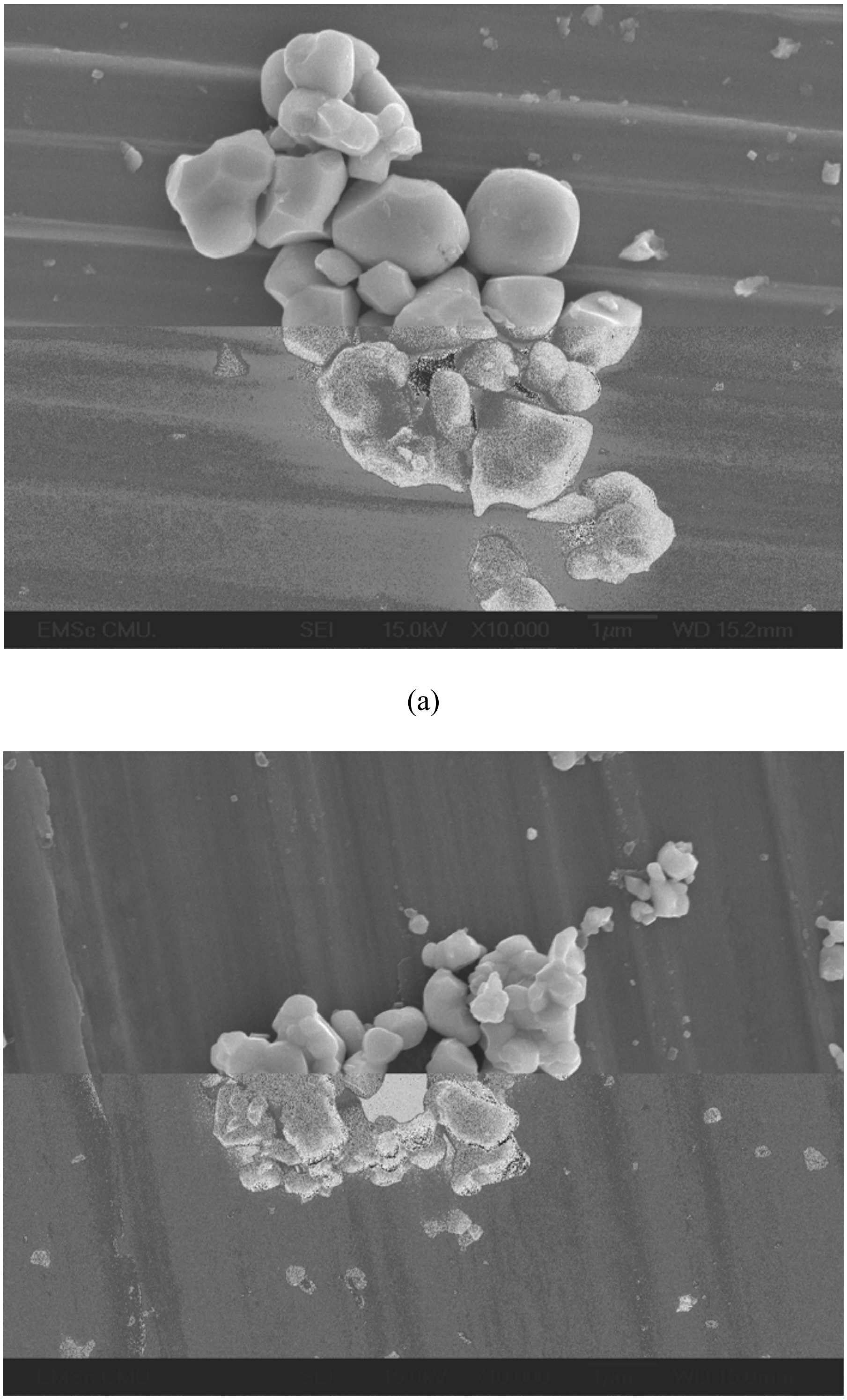

(a)

(b)

Fig. 3 SEM micrographs of PINT powders calcined at optimum temperature for (a) the conventional method and (b) the wolframite method

ภาคผนวก ข

Reprints & Menuscripts

(Part II: Ceramics in the PBZT-PMNT System)

Available online at www.sciencedirect.com

SCIENCE @ DIRECT®

Journal of the European Ceramic Society 24 (2004) 185–188

www.elsevier.com/locate/jeurceramsoc

Highly dense lead titanate ceramics from refined processing

A. Udomporn, K. Pengpat*, S. Ananta

Department of Physics, Faculty of Science, Chiang Mai University, Chiang Mai 50200, Thailand

Abstract

Lead titanate ($PbTiO_3$, PT) ceramic is a useful pyroelectric and piezoelectric material for high-temperature applications. However, it is very difficult to prepare a pure-phase and dense PT as a result of a high c/a ratio. In this study, conformable PT ceramics with 97% of the theoretical density were successfully synthesized by means of carefully controlled processing parameters that include sintering temperature, soaking time and heating/cooling rates. It can be found that these ceramics exhibit highly densified and uniform microstructure with the optimum conditions of 1225 °C sintering temperature, 2 h soaking time and 1 °C min^{-1} heating/cooling rates. Moreover, relatively inexpensive laboratory grade lead oxide (PbO) and titanium oxide (TiO_2) can be used as starting materials.

Keywords: Grain size; Microstructures; $PbTiO_3$; Powders-solid state reaction

1. Introduction

Lead titanate ($PbTiO_3$) is a ferroelectric, having a highly symmetric perovskite-type structure with a high curie temperature (T_c) of about 490 °C at which the phase transition of tetragonal ferroelectric phase ($< T_c$) to cubic paraelectric phase ($> T_c$) occurs.[1] The PT ceramic is a useful pyroelectric and piezoelectric material for high-temperature or high-frequency applications, such as non-volatile memories, infrared sensors and capacitors.[2] It is difficult to prepare a pure-phase PT ceramics with high density, as a result of a high c/a ratio of about 1.06 which gives rise to stresses in these ceramics, hence they can be easily broken and difficult to prepare in shape and size suitable for device applications.[3,4] The most widely used approach is the formation of solid-solution by adding additives, such as rare earth elements and alkaline earth elements and this is the promising technique for producing crack-free high-density materials.[5] However, the properties of PT itself are subsequently altered by the additives and as it has been known that PT has a good electrothermal property so the stoichiometric $PbTiO_3$ is still needed.[6] A lot of processing techniques for preparing the high purity and ultrafine $PbTiO_3$ powders have been extensively investigated because it is believed that these type of powders aid the formation of high density ceramics.[7] Most of the techniques were based on the chemical routes such as, sol-gel synthesis, hydrothermal reactions, coprecipitation, molten salt preparation and emulsion technique.[8–12] These chemical routes are normally complicated and expensive so they are not suitable for mass production. Therefore, the systematic study of the solid-state reaction between lead oxide and titanium oxide has been studied by Pillai and Ravindran.[13] They successfully found that the optimum sintering temperature was as low as 875 K for the formation of the single phase PT ceramic using DTA and XRD techniques. Even though the sintering temperature reported in their work was considerably low, the long period of up to 16 h dwell time was used.

In this work, the effects of thorough sintering parameters, including sintering temperatures, heating/cooling rates and soaking time on phase formation, density, microstructural development of PT ceramics have been carefully studied in order to find an optimum processing condition for forming the dense PT ceramic using conventional ceramic method.

2. Method

The PT ceramics of stoichiometric composition (PbO:TiO_2) were prepared using laboratory grade powders of 99.6% pure lead oxide (PbO) and 99.6% pure titanium oxide (TiO_2) as starting materials. After ball-milling for 24 h, drying in electric furnaces and sieving

---

* Corresponding author.
E-mail address: k_pengpat@hotmail.com (K. Pengpat).

0955-2219/$ - see front matter © 2003 Elsevier Ltd. All rights reserved.
doi:10.1016/S0955-2219(03)00605-8

with the 120 mesh, the resulting powders were calcined for 2 h at 400–1000 °C with 5 °C min^{-1} heating/cooling rate. Then various sintering conditions were employed by varying the sintering temperatures from 1185 to 1230 °C and sintering rates from 1 to 10 °C min^{-1} but dwell time was kept constant for 2 h. The bulk densities of the sintered samples were calculated using Archimedes's method. X-ray diffraction (XRD) patterns were recorded using X-ray diffractometer with CuK_α radiation. The as-received and fractured surfaces of selected ceramics were prepared for the scanning electron microscopy (SEM) analysis. The average grain sizes of the ceramics were determined using the mean linear method.

3. Results and discussions

3.1. Phase formation behaviour

Lead titanate (PT) powders were formed easily by solid-state reaction between laboratory grade powders of PbO and TiO$_2$. In this study, the formation of PT phase was initiated at the calcining temperature of 600 °C with dwell time of 2 h and heating/cooling rates of 3 °C/min, while the value reported by Pillai and Pavindran[12] was 527 °C (800 K). Additionally, the impurities of PbO phase were detected in the calcined powders of 900 and 1000 °C that may cause from the loss of vaporised PbO at high temperature. In order to confirm the complete reaction of $PbO(s)+TiO_2(s)\rightarrow PbTiO_3(s)-H$, the optimum condition of calcination used in this work was 750 °C for 2 h with heating/cooling rate of 3 °C min^{-1}.

The phase formation in the sintered ceramics of sintering temperatures ranging from 1185 to 1230 °C are presented via the X-ray diffraction as shown in Fig. 1. Table 1 presents percent shrinkage, relative density and average grain size of each ceramic sample. From Fig. 1, it can be seen that the tetragonal PT phase was formed in all PT ceramics but impurities of PbO phase were observed in the ceramics sintered at 1200 and 1220 °C while others have a high purity of PT phase. Nevertheless most of the samples suffered from severe stresses as a result of the high *c*/*a* ratio so they have broken into pieces after they were once subjected to a measurement of dielectric constant at high temperature. From Table 1,

Table 1
Percent shrinkage, relative density and grain size of PT ceramics from various sintering temperatures

Sintering temperature (°C)	Shrinkage (%)	Relative density (%)	Grain size[a] (μm)
1185	11.15	86.7	49
1190	11.03	88.9	34
1200	12.18	89.5	35
1210	12.63	92.7	27
1220	13.14	92.8	30
1225	14.06	95.4	23
1230	14.01	93.5	52

[a] The estimated precision of the grain size is ±1%.

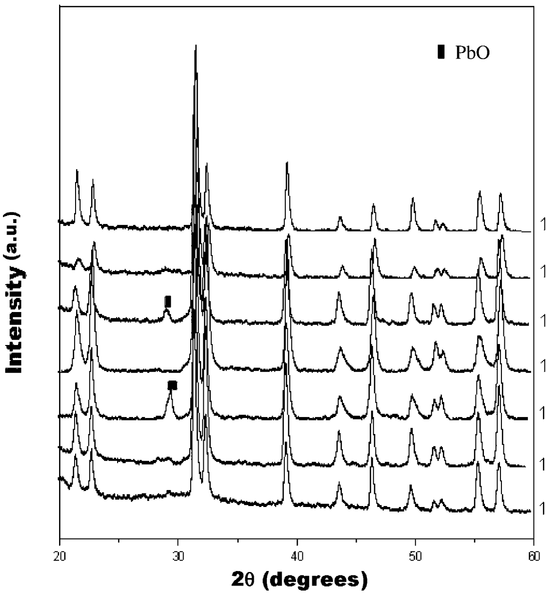

Fig. 1. The X-ray powder diffraction patterns of ceramic samples heated at different sintering temperatures with the constant dwell time of 2 h and heating/cooling rate of 3 °C min^{-1}.

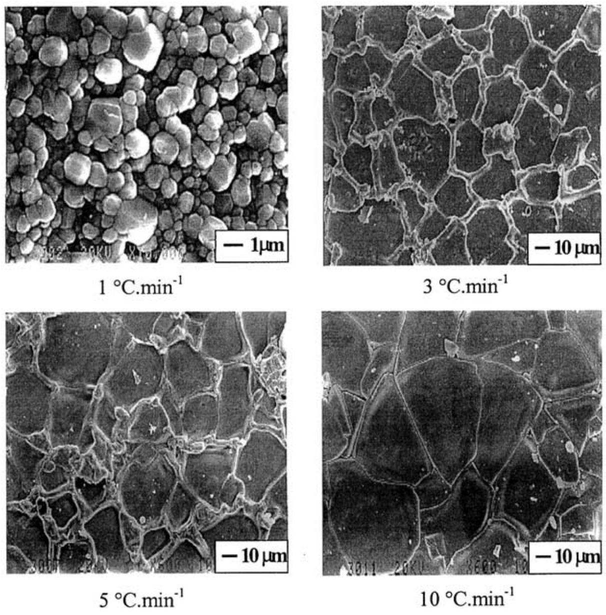

1 °C.min^{-1} 3 °C.min^{-1}

5 °C.min^{-1} 10 °C.min^{-1}

Fig. 2. The SEM images of the as-received surfaces of PbTiO$_3$ ceramics sintered at 1225 °C for 120 min with heating/cooling rate of 1 °C min^{-1} to 10 °C min^{-1}.

the ceramic sintered at 1225 °C having the highest relative density of about 95% with a smallest average grain size of about 23 µm, was of the best interest for further investigation. Therefore, another group of samples were sintered at the chosen sintering temperature of 1225 °C for 2 h with the heating/cooling rates ranging from 1 to 10 °C min^{-1}.

3.2. Densification and microstructures

Figs. 2 and 3 show the SEM images of as-received and fractured surfaces of $PbTiO_3$ ceramics, respectively. The constant sintering temperature was used for all samples at 1225 °C for 2 h while heating/cooling rates were varied from 1 °C min^{-1} to 10 °C min^{-1}. It should be noted that a pronounced second phase is segregated at the grain boundaries in the samples sintered with heating/cooling rates of 3, 5 and 10 °C min^{-1}. This second phase layer is believed to be a PbO-rich composition resulting from a liquid phase formation during the sintering process.[14,15] Table 2 contains the information of relative densities and grain sizes of the ceramics with different heating/cooling rates. It is obviously seen that heating/cooling rates are the important parameters for the development of ceramic microstructures. In that the average grain size increases with increasing heating/cooling rates as shown in Table 2. It was also found that the samples with heating/cooling rates of 3, 5 and 10 °C min^{-1} eventually burst into pieces because of the internal stresses in the ceramics as can be confirmed by the SEM images showing a loose formation of large grains in Fig. 3. Interestingly, only the samples of 1 °C min^{-1} heating/cooling rates remained with the highest relative density and smallest average grain size of about 97% and 0.6 µm, respectively. It may be assumed that, the ceramics consisting of very fine grains suffer less deformation, caused by the high value of c/a ratio, than that of the ceramics with significantly large grains. Consequently, the optimum conditions for forming the highly dense PT ceramics in this work are 1225 °C sintering temperature, 2 h dwell time and 1 °C min^{-1} heating/cooling rates. In addition, the results from Pillai and Ravindran[12] showed that single phase with average grain size of 3 µm could be formed at 602 °C (875 K) for 16 h. Even though the long period of 16 h dwell time was used, the sintering temperature was relatively low therefore the small grains could be formed in their ceramics. Conversely, high sintering temperature of 1225 °C was used in this work but the ceramics with small average grain size of 0.6 µm were still achieved. Therefore, the key parameter that controlled the grain growth here would be attributed to the slow heating rate of 1 °C min^{-1}. Conclusively, the further investigation should be carried out in order to find out exactly what inhibits grain growth in these PT ceramics while they are subjected to a long heating schedule of slow heating/cooling rates.

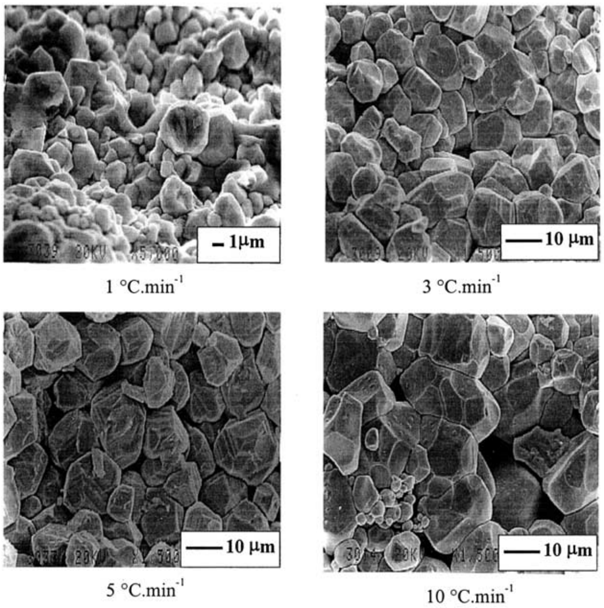

1 °C.min^{-1} 3 °C.min^{-1}

5 °C.min^{-1} 10 °C.min^{-1}

Fig. 3. The SEM images of the fractured surface of $PbTiO_3$ ceramics sintered at 1225 °C for 120 min with heating/cooling rate of 1 °C/min to 10 °C/min.

Table 2
Relative densities and grain sizes of PT ceramics sintered at 1225 °C with different heating/cooling rates

Heating/cooling rate (°C min^{-1})	Relative density (%)	Grain size (µm)[a]
1	96.8	0.6
3	94.6	23.4
5	92.1	25.9
10	92.5	30.3

[a] The estimated precision of the grain size is ±1%.

4. Conclusion

Even though the simple mixed-oxide method was used, the highly dense and stable PT ceramics were successfully formed by the careful control of processing parameters. After the thorough investigation had been performed, the optimum conditions were determined. It is found that the slow heating/cooling rates are important parameters in preparing these dense ceramics. The well defined-grain ceramics with the average grain size of about 0.6 µm could be prepared by heating them to 1225 °C using the considerably slow heating/cooling rates of 1 °C min^{-1} and dwell time of 2 h. Moreover, it was also found that the relative densities of these ceramics would be as high as 97%.